following EcoRI digestion of genomic DNA. An 8 kb fragment band corresponding to the sequence from exon 5 to exon 13 of the PGRN gene was detected in $Grn^{+/+}$ mice, a 4.3 kb fragment corresponding to PGK-Neo-bpA and endogenous genomic sequences in $Grn^{-/-}$ mice and both 8 and 4.3 kb bands in $Grn^{+/-}$ mice. To further examine the expression of PGRN mRNA, RT-PCR was performed. The 212 bp expected bands were detected in the epididymis, testis, lung and liver when cDNA from $Grn^{+/+}$ mice was used as the template (Fig. 1D). Weak signals were also detected in the brain and kidney of $Grn^{+/+}$ mice. However, no bands were detected in any examined tissues obtained from $Grn^{-/-}$ mice. A 516 bp band corresponding to β-actin was amplified in all tissues examined from both the $Grn^{+/+}$ and $Grn^{-/-}$ mice.

The genotypes of 442 offspring obtained by matings between $Grn^{+/-}$ male and female mice were 28.1% (124/442) $Grn^{+/+}$, 49.3% (218/442) $Grn^{+/-}$ and 22.6% (100/442) $Grn^{-/-}$, which matched with Mendel's laws of inheritance. The mean litter size from $Grn^{-/-}$ pairs was 6.3 ± 0.3 (mean ± S.E.M., $n = 10$), which was not significantly different from that of $Grn^{+/+}$ pairs (7.9 ± 0.2, $n = 18$). The mean number of weaned pups at 30 days of age was also not significantly different between $Grn^{+/+}$ parents (6.9 ± 0.2, $n = 15$) and $Grn^{-/-}$ parents (4.7 ± 0.3, $n = 9$).

3.2. Male sexual behaviour

The data regarding male sexual behaviour are shown in Fig. 2. The latency and frequency of mount and intromission were not significantly different among the three genotypes throughout the three trials (Fig. 2A and B). However, ejaculation incidence was lower in $Grn^{-/-}$ mice compared to $Grn^{+/+}$ and $Grn^{+/-}$ mice throughout the trials and was significantly different at the second trial (Fig. 2C, left). The percentage of mice displaying ejaculation at least once over the three trials was also significantly lower in $Grn^{-/-}$ mice than that in $Grn^{+/+}$ mice (Fig. 2C, right). Since aggressive behaviours toward females were observed dur-

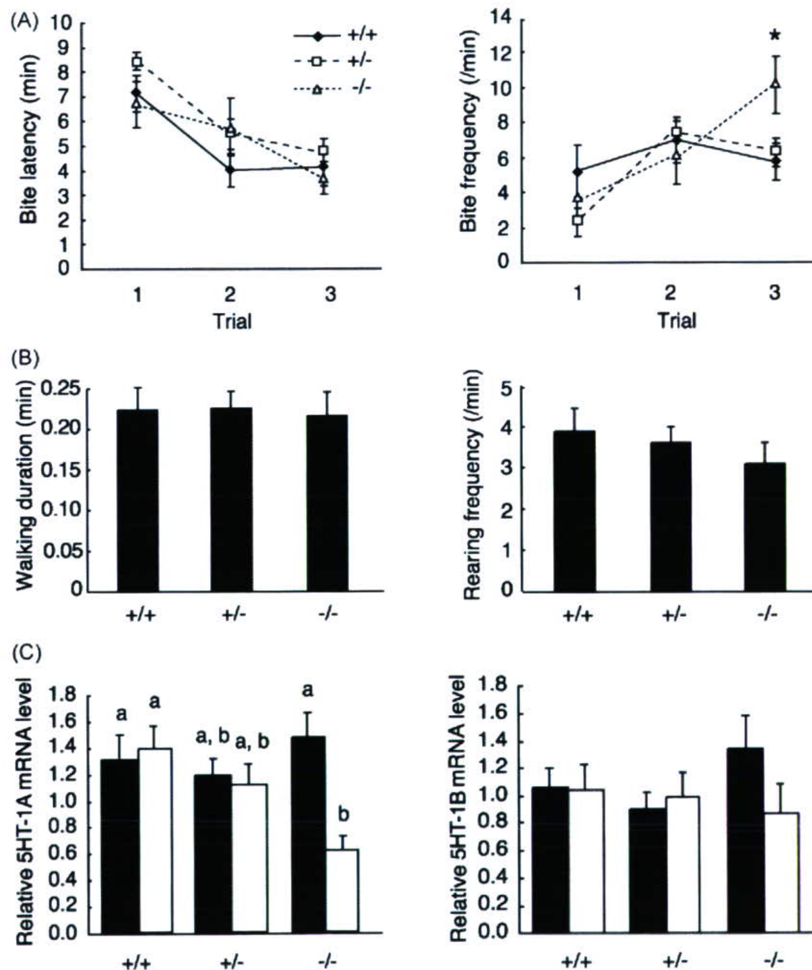

Fig. 3. Analysis of aggressive behaviour. The resident–intruder paradigm was used to assess inter-male aggression. Each male was tested against a male A/J intruder for 5–15 min and behaviour recorded. Tests were repeated three times for each male ($n = 14$ for $Grn^{+/+}$, $n = 23$ for $Grn^{+/-}$, $n = 12$ for $Grn^{-/-}$). (A) Latency (left) and frequency (right) of biting attack. Each symbol and vertical bar represents the mean and S.E.M., respectively. $^{*}p < 0.05$, two-way ANOVA followed by Fisher's PLSD test, compared to $Grn^{+/+}$, $Grn^{+/-}$. (B) Duration of walking (left) and frequency of rearing (right) during 5 min of the first aggressive behaviour test. Each column and vertical bar represents the mean and S.E.M., respectively. (C) Expression of 5-HT1A (left) and 1B (right) mRNA in the hippocampus. Relative mRNA levels of 5-HT1A and 1B to HPRT in the hippocampus of mice with (open column) or without aggressive encounters (closed column) were determined by real-time PCR. Each column and vertical bar represents the mean and S.E.M., respectively ($n = 9$ for each experimental group). The values with different letters are significantly different ($p < 0.05$, two-way ANOVA followed by Fisher's PLSD test).

ing the sexual behaviour tests, the number of aggressive bouts was also counted in this experiment. Although the total number of aggressive bouts over the three trials was not statistically different among the three genotypes, the number was much larger in $Grn^{-/-}$ than $Grn^{+/+}$ mice, while that of $Grn^{+/-}$ mice was intermediate between the two (Fig. 2D). There was no significant difference in serum testosterone concentrations in males among the three genotypes (Fig. 2E).

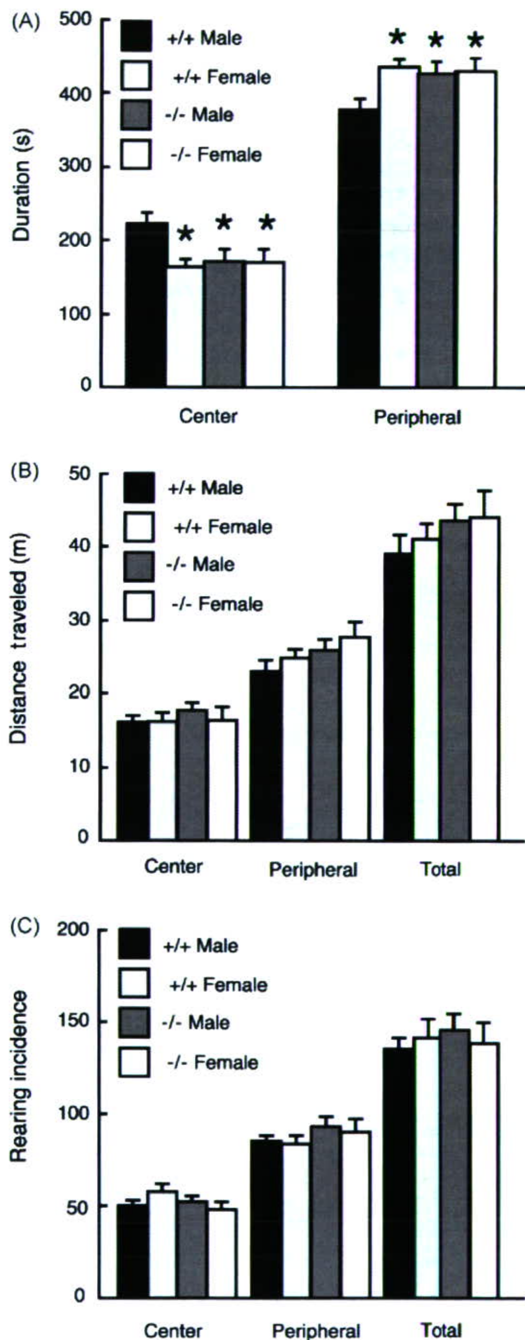

Fig. 4. Analysis of anxiety. Each mouse was placed in the center of the square (open field) and its behaviour was recorded for 10 min. (A) Duration in center, (B) distance traveled and (C) incidence of rearings of male and female $Grn^{+/+}$ and $Grn^{-/-}$ mice. Each column and vertical bar represents the mean and S.E.M., respectively ($n = 13$ for $Grn^{+/+}$ male, $n = 22$ for $Grn^{+/+}$ female, $n = 22$ for $Grn^{-/-}$ male and $n = 14$ for $Grn^{-/-}$ female). $^{*}p < 0.05$, ANOVA followed by Student's t-test, compared to $Grn^{+/+}$ male.

3.3. Aggression

Since $Grn^{-/-}$ mice exhibited prominent, although not significant, aggressive behaviour towards females during the male sexual behaviour test as mentioned above, we evaluated the rate of offensive inter-male fighting by means of a resident–intruder paradigm. As shown in Fig. 3A (left), the latency to the first biting attack tended to be shorter with each trial, although there was no significant difference among the three genotypes. However, as shown in Fig. 3A (right), the frequency of biting attacks in $Grn^{-/-}$ mice was significantly higher than that of $Grn^{+/+}$ and $Grn^{+/-}$ mice at the third trial, although the frequency did not differ among the genotypes in the first and second trials. The duration of walking and the number of rearings, which were recorded during the first trial to evaluate locomotor activity, were not significantly different between the genotypes (Fig. 3B). Since PGRN-deficient mice exhibited enhanced aggressiveness after repeated encounters with intruders, we evaluated the mRNA expression of the serotonergic receptors 5-HT1A and 1B in the hippocampus, which could be related to inhibition of aggression and anxiety, after three instances of aggressive encounters. As shown in Fig. 3C (left), the mRNA expression of 5-HT1A was significantly decreased in the hippocampus of $Grn^{-/-}$ mice that experienced aggressive encounters, while that in $Grn^{+/+}$ and $Grn^{+/-}$ mice remained unchanged. The expression of 5-HT1B mRNA also tended to be decreased following aggressive encounters in $Grn^{-/-}$ mice, but the difference was not significant (Fig. 3C, right). There was no significant difference in both 5-HT1A and 1B mRNA levels among genotypes of mice that did not encounter intruders.

3.4. Anxiety

The levels of anxiety in PGRN-deficient mice were evaluated using the open field test. As shown Fig. 4A, female $Grn^{+/+}$ mice spent significantly less time in the center of the square compared to male $Grn^{+/+}$ mice, although sex difference in the duration staying in the center was not observed in $Grn^{-/-}$ mice. In addition, male $Grn^{-/-}$ mice male spent significantly less time in the center compared to male $Grn^{+/+}$ mice. The distances traveled (Fig. 4B) and incidence of rearing (Fig. 4C) in the center, peripheral zone and the total were not different between sex nor genotypes.

4. Discussion

In the present study, we generated mice with targeted disruption of the PGRN gene to investigate the possible role of PGRN/granulins in the brain. Since it is reported that PGRN is expressed in the acrosome of the sperm [3] and oocytes [47] and that PGRN modulates the development of early embryos *in vitro* [19], we suspected that $Grn^{-/-}$ mice might be fetal lethal or exhibit disorders in reproductive function. However, they were fertile, and both litter size and the number of weaned pups were not different between $Grn^{+/+}$ pairs and $Grn^{-/-}$ pairs. It is therefore suggested that PGRN is not necessarily a critical factor

for fertilization and development, especially *in vivo*, in which numerous factors are likely to be involved.

4.1. Attenuation of sexual behaviour

In the male sexual behaviour analysis, the latency and frequency of mount and intromission were not significantly different among the three genotypes, yet ejaculation incidence and the number of mice displaying ejaculation were significantly lower in $Grn^{-/-}$ mice compared to $Grn^{+/+}$ and $Grn^{+/-}$ males. We have previously shown that neonatal treatment of the male rat brain with antisense oligodeoxynucleotides for the PGRN gene suppressed all mount, intromission and ejaculation [46]. The precise reason for this discrepancy is unknown; however, the processes of brain sexual differentiation may vary between rats and mice. The dogma that estrogens converted from androgens masculinize the neonatal brain is mostly derived from the results from rat experiments, but this may not be the case for mice. This fact has come to light recently with the generation of many kinds of knockout (KO) mice in the research fields of reproduction and neuroscience. For example, data from aromatase KO [5] and estrogen receptor (ER) KO [53] male mice suggest that the lack of exposure to, or receptors for, estrogens during development impairs, but does not necessarily eliminate, expression of male sexual behaviour in adulthood. This may be one of the reasons why complete suppression of male sexual behaviour was not seen in the $Grn^{-/-}$ mice.

The mechanisms for inducing ejaculation are known to differ from those of mount and intromission. Although the medial preoptic area and medial amygdala are regarded as the main controlling sites of male sexual behaviour [36], ejaculation is also mediated by the spinal control center [15]. In addition, the form of the steroid that activates the behaviour seems different [37]. When 5α-dihydrotestosterone (DHT) or 17β-estradiol (E_2) was administered to castrated male mice, E_2 restored mount and intromission to the same extent as DHT, but ejaculation was not restored to the same extent by E_2 compared to DHT. Furthermore, even in castrated male androgen receptor (AR) KO mice, E_2 restored mount and intromission to some extent, but not ejaculation [40]. These observations suggest that mount and intromission can be activated by estrogens as well as androgens, but that ejaculation is activated through AR-mediated processes. In $Grn^{-/-}$ mice, the neuronal structure(s) inducing ejaculation in response to androgens may not be normally differentiated. Since serum testosterone levels were not different among genotypes, PGRN does not seem to affect the neuroendocrine system controlling gonadotropin secretion.

4.2. Augmentation of aggression and anxiety

During the male sexual behaviour test, aggressive behaviour toward females was noticed in $Grn^{-/-}$ mice. Moreover, the total number of aggressive bouts over the three trials tended to be higher in $Grn^{-/-}$ than in $Grn^{+/+}$ or $Grn^{+/-}$ mice. We therefore further investigated inter-male aggression by means of the resident–intruder paradigm. Although bite latency was not different among the three genotypes in any of the trials, the frequency of biting attacks was significantly higher at the third trial in $Grn^{-/-}$ mice compared with $Grn^{+/+}$ and $Grn^{+/-}$ littermates. These changes in aggressive behaviour were well correlated with changes in mRNA expression of serotonergic receptors in the hippocampus, which were involved in reducing aggression and anxiety [18,51]. We observed that it took longer for $Grn^{-/-}$ mice to stop attacking once they started regardless of the intruder's submission, which could be regarded as "impulsive" aggression.

Territorial aggression, as assessed by the resident–intruder paradigm, is regarded as one of the male-dominant behaviours [37], and therefore, the present results can be interpreted such that the brain of male $Grn^{-/-}$ mice could be "hyper-masculinized". This conflicts with our above-mentioned notion that PGRN/granulins mediate the masculinizing effects of sex steroids on the brain. While it is difficult to reconcile this discrepancy, we consider the increased aggression in $Grn^{-/-}$ mice to be related to an increase in anxiety rather than male-type sex role behaviour. This is because $Grn^{-/-}$ mice showed aggressive behaviours toward not only males, but also females, and they displayed a significant increase in the level of anxiety in the open field test. In addition, elevated anxiety is often associated with an increase in aggression [26]. It is of interest that females displayed higher levels of anxiety than males in our open field experimental paradigm. Taken together, it is probable that the enhancement of aggression in male PGRN-deficient mice is derived from elevated anxiety due to insufficient masculinization of the brain. Alternatively, female-directed aggression during mating test as well as increased aggression only after repeated exposure to an intruder may suggest an impairment in gender and/or social recognition. This would be in agreement with results from the ERα and ERβ KO mice [12], and also support that estrogen actions in the brain are at least partially mediated by PGRN.

4.3. Possible alteration in the serotonergic system

As mentioned above, 5-HT1A mRNA levels were significantly decreased in the hippocampus of PGRN-deficient mice that experienced aggressive encounters. At present, the mechanism underlying this phenomenon is unclear, but since stress is one of the factors inducing aggressive behaviour [31,49] and exposure to acute stress reduces mRNA expression of 5-HT1A in the hippocampus [29], the serotonergic system of PGRN-deficient mice may be more susceptible to stress, e.g., by encounter with unfamiliar situations, including the presence of intruders.

PGRN/granulins may be related to the organization and/or activation of the serotonergic system in the brain. Alterations in serotonergic neurotransmission have been found in many of the KO mice that display unusual aggressive behaviour [10,39,41]. Serotonergic systems are reported to retain their plasticity after birth in the neonatal period [52] or even up to the weaning period [27], and their distribution and density are influenced by internal environmental facilitators, such as nourishment and growth factors. Moreover, the brain serotonergic system is under the influence of sex steroids [13,14,44,55]. Since PGRN functions as a growth factor the expression of which is regulated by sex

steroids [30,48], it is probable that PGRN mediates the effects of sex steroids on the serotonergic system. Since some of the phenotypes displayed by $Grn^{-/-}$ mice are similar to those of βERKO mice, which have longer ejaculation latency [50], higher aggressiveness described as "impulsive" [35], and lower serotonin content in several brain regions [25], PGRN gene expression may be modulated through ERβ rather than ERα.

Recently, PGRN gene mutations were identified as the responsible factor for familial FTD [4,16]. FTD is characterized by progressive changes in behaviour, personality and language with atrophy of the frontal and temporal lobe of the cerebral cortex [34]. Emotional disturbances, such as dysthymia, anxiety and anger or aggressive behaviour have been also reported in FTD patients [33]. These behavioural and emotional changes may result from the deficits of the serotonergic system, since several studies have indicated the efficacy of treatment with selective serotonin-reuptake inhibitors [21,24] and 5-HT receptor agonists [28] for these symptoms. In addition, decreased levels of serotonin receptors in the cerebral cortices of FTD patients have been reported [20,38]. These observations also support the involvement of PGRN/granulins in modulating the brain serotonergic system.

In conclusion, the present study suggests that PGRN is involved in exhibiting some sexual dimorphic behaviour at least partially by modulating the brain serotonergic system. Although further studies are needed to clarify the precise mechanisms underlying changes in behavioural phenotypes in PGRN-deficient mice, PGRN may play multiple roles in the brain including sexual differentiation at the perinatal period, neurogenesis in the adult hippocampus [11] and the onset of FTD at old ages [4,16].

Acknowledgements

Y.K. and S.C. equally contributed to this work. This work was supported by Grants-in-Aid for Scientific Research (17208025, 17052003 to M.N.) from the Japan Society for the Promotion of Science and the Ministry of Education, Culture, Sports, Science and Technology of Japan.

References

[1] Arnold AP, Gorski RA. Gonadal steroid induction of structural sex differences in the central nervous system. Ann Rev Neurosci 1984;7:413–42.

[2] Asano M, Furukawa K, Kido M, Matsumoto S, Umesaki Y, Kochibe N, et al. Growth retardation and early death of β-1,4-galactosyltransferase knockout mice with augmented proliferation and abnormal differentiation of epithelial cells. EMBO J 1997;16:1850–7.

[3] Baba T, Nemoto H, Watanabe K, Arai Y, Gerton GL. Exon/intron organization of the gene encoding the mouse epithelin/granulin precursor (acrogranin). Eur J Biochem 1993;322:89–94.

[4] Baker M, Mackenzie IR, Pickering-Brown SM, Gass J, Rademakers R, Lindholm C, et al. Mutations in progranulin cause tau-negative frontotemporal dementia linked to chromosome 17. Nature 2006;442:916–9.

[5] Bakker J, Honda S, Harada N, Balthazart J. Restoration of male sexual behavior by adult exogenous estrogens in male aromatase knockout mice. Horm Behav 2004;46:1–10.

[6] Bateman A, Belcourt D, Bennett H, Lazure C, Solomon S. Granulins, a novel class of peptides from leukocytes. Biochem Biophys Res Commun 1990;173:1161–8.

[7] Bateman A, Bennett HPJ. Granulins: the structure and function of an emerging family of growth factors. J Endocrinol 1998;158:145–51.

[8] Bhandari V, Palfree RG, Bateman A. Isolation and sequence of the granulin precursor cDNA from human bone marrow reveals tandem cysteine-rich granulin domains. Proc Natl Acad Sci USA 1992;89:1715–9.

[9] Bhandari V, Giaid A, Bateman A. The complementary deoxyribonucleic acid sequence, tissue distribution, and cellular localization of the rat granulin precursor. Endocrinology 1993;133:2682–9.

[10] Cases O, Seif I, Grimsby J, Gaspar P, Chen K, Pournin S, et al. Aggressive behavior and altered amounts of brain serotonin and norepinephrine in mice lacking MAO-A. Science 1995;268:1763–6.

[11] Chiba S, Suzuki M, Yamanouchi K, Nishihara M. Involvement of granulin in estrogen-induced neurogenesis in the adult rat hippocampus. J Reprod Dev 2007;53:297–307.

[12] Choleris E, Gustafsson JA, Korach KS, Muglia LJ, Pfaff DW, Ogawa S. An estrogen-dependent four-gene micronet regulating social recognition: a study with oxytocin and estrogen receptor-α and -β knockout mice. Proc Natl Acad Sci USA 2003;100:6192–7.

[13] Cologer-Clifford A, Simon NG, Richter ML, Smoluk SA, Lu S. Androgens and estrogens modulate 5-HT1A and 5-HT1B agonist effects on aggression. Physiol Behav 1999;65:823–8.

[14] Connell S, Karikari C, Hohmann CF. Sex-specific development of cortical monoamine levels in mouse. Dev Brain Res 2004;151:187–91.

[15] Coolen LM, Allard J, Truitt WA, McKenna KE. Central regulation of ejaculation. Physiol Behav 2004;83:203–15.

[16] Cruts M, Gijselinck I, van der Zee J, Engelborghs S, Wils H, Pirici D, et al. Null mutation in progranulin cause ubiquitin-positive frontotemporal dementia linked to chromosome 17q21. Nature 2006;442:920–4.

[17] Daniel R, He Z, Carmichael KP, Halper J, Bateman A. Cellular localization of gene expression for progranulin. J Histochem Cytochem 2000;48:999–1009.

[18] De Almeida RMM, Rosa MM, Santos DM, Saft DM, Benini Q, Miczek KA. 5-HT1B receptors, ventral orbitofrontal cortex, and aggressive behavior in mice. Psychopharmacology 2006;185:441–50.

[19] Diaz-Cueto L, Stein P, Jacobs A, Schultz RM, Gerton GL. Modulation of mouse preimplantation embryo development by acrogranin (epithelin/granulin precursor). Dev Biol 2000;217:406–18.

[20] Franceschi M, Anchisi D, Pelati O, Zuffi M, Matarrese M, Moresco RM, et al. Glucose metabolism and serotonin receptors in the frontotemporal lobe degeneration. Ann Neurol 2005;57:216–25.

[21] Huey ED, Putnam KT, Grafman J. A systematic review of neurotransmitter deficits and treatments in frontotemporal dementia. Neurology 2006;66:17–22.

[22] Hooper M, Hardy K, Handyside A, Hunter S, Monk M. HPRT-deficient (Lech–Nyhan) mouse embryos derived from germline colonization by cultured cells. Nature 1987;326:292–5.

[23] Horai R, Asano M, Sudo K, Kanuka H, Suzuki M, Nishihara M, et al. Production of mice deficient in genes for interleukin (IL)-1α, IL-1β, IL-1α/β, and IL-1 receptor antagonist shows that IL-1 β is crucial in turpentine-induced fever development and glucocorticoid secretion. J Exp Med 1998;187:1463–75.

[24] Ikeda M, Shigenobu K, Fukuhara R, Hokoishi K, Maki N, Nebu A, et al. Efficacy of fluvoxamine as a treatment for behavioral symptoms in frontotemporal lobar degeneration patients. Dement Geriatr Cogn Disord 2004;17:117–21.

[25] Imwalle D, Gustafsson J, Rissman E. Lack of functional estrogen receptor β influences anxiety behavior and serotonin content in female mice. Physiol Behav 2005;84:157–63.

[26] Kikusui T, Takeuchi Y, Mori Y. Early weaning induces anxiety and aggression in adult mice. Physiol Behav 2004;81:37–42.

[27] Kinney GG, Vogel GW, Feng P. Decreased dorsal raphe nucleus neuronal activity in adult chloral hydrate anesthetized rats following neonatal clomipramine treatment: implications for endogenous depression. Brain Res 1997;756:68–75.

[28] Lebert F, Stekke W, Hasenbroekx C, Pasquier F. Frontotemporal dementia: a randomised, controlled trial with trazodone. Dement Geriatr Cogn Disord 2004;17:355–9.

[29] Lopez JF, Liberzon I, Vazquez DM, Young EA, Watson SJ. Serotonin 1A receptor messenger RNA regulation in the hippocampus after acute stress. Biol Psychiatry 1999;45:934–7.

[30] Lu R, Serrero G. Mediation of estrogen mitogenic effect in human breast cancer MCF-7 cells by PC-cell-derived growth factor (PCDGF/granulin precursor). Proc Natl Acad Sci USA 2001;98:142–7.

[31] Matsumoto K, Pinna G, Puia G, Guidotti A, Costa E. Social isolation stress-induced aggression in mice: a model to study the pharmacology of neurosteroidogenesis. Stress 2005;8:85–93.

[32] McEwen BS, Lieberburg I, Chaptal C, Krey LC. Aromatization: important for sexual differentiation of the neonatal rat brain. Horm Behav 1977;9:249–63.

[33] Mendez MF, McMurtray A, Chen AK, Shapira JS, Mishkin F, Miller BL. Functional neuroimaging and presenting psychiatric features in frontotemporal dementia. J Neurol Neurosurg Psychiatry 2006;77:4–7.

[34] Neary D, Snowden J, Mann D. Frontotemporal dementia. Lancet Neurol 2005;4:771–80.

[35] Ogawa S, Chan J, Chester AE, Gustafsson JA, Korach KS, Pfaff DW. Survival of reproductive behaviors in estrogen receptor β gene-deficient (βERKO) male and female mice. Proc Natl Acad Sci USA 1999;96:12887–92.

[36] Paredes RG, Baum MJ. Role of the medial preoptic area/anterior hypothalamus in the control of masculine sexual behavior. Annu Rev Sex Res 1997;8:68–101.

[37] Pfaff DW. Hormonal processes in the development and expression of aggressive behavior. In: Pfaff DW, editor. Hormones, brain and behavior, vol. 1. New York: Academic Press; 2002. p. 339–92.

[38] Procter AW, Qurne M, Francis PT. Neurochemical features of frontotemporal dementia. Dement Geriatr Cogn Disord 1999;10(Suppl. 1):80–4.

[39] Sallinen J, Haapalinna A, Viitamaa T, Kobilka BK, Scheinin M, Adrenergic. α2c Receptors modulate the acoustic startle reflex, prepulse inhibition and aggression in mice. J Neurosci 1998;18:3035–42.

[40] Sato T, Matsumoto T, Kawano H, Watanabe T, Uematsu Y, Sekine K, et al. Brain masculinization requires androgen receptor function. Proc Natl Acad Sci USA 2004;101:1673–8.

[41] Saudou F, Amara DA, Dierich A, LeMeur M, Ramboz S, Segu L, et al. Enhanced aggressive behavior in mice lacking 5-HT_{1B} receptor. Science 1994;265:1875–8.

[42] Shoyab M, McDonald VL, Byles C, Todaro GJ, Plowman GD. Epithelins 1 and 2: isolation and characterization of two cysteine-rich growth-modulating peptides. Proc Natl Acad Sci USA 1990;87:7912–6.

[43] Soriano P, Montogomery C, Geske R, Bradley A. Targeted disruption of the c-src proto-oncogene leads to osteopetrosis in mice. Cell 1991;64:693–702.

[44] Summer BE, Fink G. Testosterone as well as estrogen increases serotonin 2A receptor mRNA and binding site densities in the male rat brain. Mol Brain Res 1998;59:205–14.

[45] Suzuki M, Yoshida Y, Nishihara M, Takahashi M. Identification of a sex steroid-inducible gene in the neonatal rat hypothalamus. Neurosci Lett 1998;242:127–30.

[46] Suzuki M, Bannai M, Matsumuro M, Furuhata Y, Ikemura R, Kuranaga E, et al. Suppression of copulatory behavior by intracerebroventricular infusion of antisense oligodeoxynucleotide of granulin in neonatal male rats. Physiol Behav 2000;68:707–13.

[47] Suzuki M, Matsumuro M, Hirabayashi K, Ogawara M, Takahashi M, Nishihara M. Oocyte-specific expression of granulin precursor (acrogranin) in rat ovary. J Reprod Dev 2000;46:271–7.

[48] Suzuki M, Yonezawa T, Fujioka H, Matuamuro M, Nishihara M. Induction of granulin precursor gene expression by estrogen treatment in neonatal rat hypothalamus. Neurosci Lett 2001;297:199–202.

[49] Tedeschi RE, Tedeschi DH, Mucha A, Cook L, Mattis PA, Fellows EJ. Effects of various centrally acting drugs on fighting behavior of mice. J Pharmacol Exp Ther 1959;125:28–34.

[50] Temple JL, Scordalakes EM, Bodo C, Gustafsson JA, Rissman EF. Lack of functional estrogen receptor β gene disrupts pubertal male sexual behavior. Horm Behav 2003;44:427–34.

[51] van Riel D, Miijer OC, Veenem AH, Joels M. Hippocampal serotonin responses in short and long attack latency mice. J Neuroendocrinol 2002;14:234–9.

[52] Vitalis T, Cases O, Callebert J, Launay JM, Price DJ, Seif I, et al. Effects of monoamine oxidase A inhibition on barrel formation in the mouse somatosensory cortex: determination of a sensitive developmental period. J Comp Neurol 1998;393:169–84.

[53] Wersinger SR, Sannen K, Villalba C, Lubahn DB, Rissman EF, De Vries GJ. Masculine sexual behavior is disrupted in male and female mice lacking a functional estrogen receptor α gene. Horm Behav 1997;32:176–83.

[54] Yagi T, Nada S, Watanabe N, Tamemoto H, Kohmura N, Ikawa Y, et al. A novel negative selection for homologous recombinants using diphtheria toxin A fragment gene. Anal Biochem 1993;214:77–86.

[55] Zhang L, Ma W, Barker JL, Rubinow DR. Sex difference in expression of serotonin receptors (subtype 1A and 2A) in rat brain: a possible role of testosterone. Neuroscience 1999;94:251–9.

European Journal of Neuroscience, Vol. 26, pp. 2269–2278, 2007 doi:10.1111/j.1460-9568.2007.05829.x

Involvement of protein-tyrosine phosphatase PTPMEG in motor learning and cerebellar long-term depression

Shin-ichiro Kina,[1] Tohru Tezuka,[1] Shinji Kusakawa,[2] Yasushi Kishimoto,[3,4,*] Sho Kakizawa,[5] Koichi Hashimoto,[3,4] Miho Ohsugi,[1] Yuji Kiyama,[2] Reiko Horai,[6] Katsuko Sudo,[6,†] Shigeru Kakuta,[6] Yoichiro Iwakura,[6] Masamitsu Iino,[5] Masanobu Kano,[3,4] Toshiya Manabe[2,7] and Tadashi Yamamoto[1]

[1]Division of Oncology, Department of Cancer Biology, Institute of Medical Science, University of Tokyo, Minato-ku, Tokyo, 108-8639, Japan
[2]Division of Neuronal Network, Department of Basic Medical Sciences, Institute of Medical Science, University of Tokyo, Minato-ku, Tokyo, 108-8639, Japan
[3]Department of Cellular Neurophysiology, Graduate School of Medical Science, Kanazawa University, Kanazawa, 920-8640, Japan
[4]Department of Cellular Neuroscience, Graduate School of Medicine, Osaka University, Suita, 565-0871, Japan
[5]Department of Cellular and Molecular Pharmacology, Graduate School of Medicine, University of Tokyo, Bunkyo-ku, Tokyo, 113-0033, Japan
[6]Division of Cell Biology, Center for Experimental Medicine, Institute of Medical Science, University of Tokyo, Minato-ku, Tokyo, 108-8639, Japan
[7]CREST and RISTEX, Japan Science and Technology Agency

Keywords: cerebellum, eyeblink conditioning, knockout mice, phosphorylation, Purkinje cells

Abstract

Although protein-tyrosine phosphorylation is important for hippocampus-dependent learning, its role in cerebellum-dependent learning remains unclear. We previously found that PTPMEG, a cytoplasmic protein-tyrosine phosphatase expressed in Purkinje cells (PCs), bound to the carboxyl-terminus of the glutamate receptor δ2 via the postsynaptic density-95/discs-large/ZO-1 domain of PTPMEG. In the present study, we generated PTPMEG-knockout (KO) mice, and addressed whether PTPMEG is involved in cerebellar plasticity and cerebellum-dependent learning. The structure of the cerebellum in PTPMEG-KO mice appeared grossly normal. However, we found that PTPMEG-KO mice showed severe impairment in the accelerated rotarod test. These mice also exhibited impairment in rapid acquisition of the cerebellum-dependent delay eyeblink conditioning, in which conditioned stimulus (450-ms tone) and unconditioned stimulus (100-ms periorbital electrical shock) were co-terminated. Moreover, long-term depression at parallel fiber–PC synapses was significantly attenuated in these mice. Developmental elimination of surplus climbing fibers and the physiological properties of excitatory synaptic inputs to PCs appeared normal in PTPMEG-KO mice. These results suggest that tyrosine dephosphorylation events regulated by PTPMEG are important for both motor learning and cerebellar synaptic plasticity.

Introduction

The mammalian cerebellum is important for motor coordination, sensorimotor integration, motor learning and timing to non-motor functions such as cognition (Schmahmann & Sherman, 1998; Ito, 2002; Boyden *et al.*, 2004; Swinny *et al.*, 2005). Motor coordination is a smooth execution of compound movements, whereas motor learning is a process of improving the accuracy and/or efficiency of movements (Ito, 2002; Swinny *et al.*, 2005). Purkinje cells (PCs) provide the sole output from the cerebellar cortex. They receive two distinct excitatory inputs: one from parallel fibers (PFs), the bifurcated axons of granule cells; and the other from climbing fibers (CFs) that originate in the inferior olive. Modulation of PC activity by PF- and CF-inputs contributes to both motor coordination and motor learning.

Correspondence: Dr T. Yamamoto, as above.
E-mail: tyamamot@ims.u-tokyo.ac.jp

**Present address*: Department of Neurobiophysics, Graduate School of Pharmaceutical Sciences at Kagawa campus, Tokushima Bunri University, Sanuki, 769-2193, Japan.

†Present address: Animal Research Center, Tokyo Medical University, Tokyo, 160-8402, Japan.

Received 15 January 2007, revised 14 August 2007, accepted 16 August 2007

Cerebellar long-term depression (LTD) at PF–PC synapses is reported to underlie several forms of cerebellum-dependent motor learning, such as classical eyeblink conditioning and adaptation of the vestibulo-ocular reflex (Ito, 2002). In cerebellar LTD, a persistent and input-specific attenuation of the PF–PC synaptic efficacy is induced when PF- and CF-inputs to PC are stimulated together at low frequencies. Cerebellar LTD requires three types of glutamate receptors (GluRs) in PCs, which are metabotropic GluR1 (mGluR1), GluRδ2 and α-amino-3-hydroxy-5-methyl-4-isoxazolepropionic acid type receptors (AMPARs; Ito, 2002). Stimulation of mGluR1 leads to protein kinase C (PKC)-mediated phosphorylation of the AMPAR subunit GluR2. This phosphorylation results in endocytosis of AMPARs and downregulation of AMPAR-mediated synaptic transmission (Chung *et al.*, 2003; Steinberg *et al.*, 2006). GluRδ2 is involved in AMPAR trafficking (Hirai *et al.*, 2003), and several GluRδ2-interacting proteins have been identified (Yuzaki, 2004; Yawata *et al.*, 2006). However, the molecular mechanism by which GluRδ2 participates in cerebellar LTD and motor learning is largely unknown. In addition to serine/threonine phosphorylation, tyrosine phosphorylation events are also implicated in cerebellar LTD and motor learning (Castro-Alamancos & Torres-Aleman, 1994; Boxall

© The Authors (2007). Journal Compilation © Federation of European Neuroscience Societies and Blackwell Publishing Ltd

et al., 1996; Wang & Linden, 2000). For example, insulin/insulin-like growth factor-I can induce LTD in PCs (Wang & Linden, 2000). Lavendustin A and herbimycin A, inhibitors of protein-tyrosine kinases (PTKs), suppress cerebellar LTD (Boxall *et al.*, 1996). However, the roles of tyrosine phosphorylation events in cerebellar LTD and motor learning remain to be established.

PTPMEG/PTPN4 is a cytoplasmic protein-tyrosine phosphatase (PTP) containing protein 4.1 and Ezrin/Radixin/Moesin (FERM) and postsynaptic density-95/discs-large/ZO-1 (PDZ) domains, which was originally identified from a megakaryoblastic cell line (Gu *et al.*, 1991). Although overexpression of PTPMEG in COS-7 cells inhibits cell proliferation (Gu *et al.*, 1996), physiological roles of PTPMEG have not been elucidated. We previously showed that PTPMEG mRNA was expressed at high levels in PCs and the thalamus, and that PTPMEG bound to the carboxyl-terminus of GluRδ2 via the PDZ domain of PTPMEG (Hironaka *et al.*, 2000). Because GluRδ2 is essential for both cerebellar development including synapse formation and cerebellar function, such as motor coordination and motor learning (Kashiwabuchi *et al.*, 1995; Kishimoto *et al.*, 2001c; Yuzaki, 2004), PTPMEG may also play a role in the cerebellar function. In this study, we generated PTPMEG-knockout (KO) mice, and found that these mice showed impairment in memory formation of motor learning and cerebellar LTD at PF–PC synapses.

Materials and methods

Generation of PTPMEG-KO mice

P1 clones carrying PTPMEG genomic sequences were obtained from a mouse ES-129/SvJ genomic library. The targeting vector was constructed, in which a Tau-LacZ cassette (Callahan & Thomas, 1994) and a PGK-neo expression cassette were inserted at the translational initiation codon of the PTPMEG gene. The linearized vector was electroporated into E14 ES cells, and G418-resistant clones with the anticipated homologous recombination were screened by polymerase chain reaction and Southern blotting. Chimeric mice were generated by an aggregation method. Male chimeras were mated with C57BL/6J females to obtain PTPMEG heterozygous mice (F1) with a 50% pure C57BL/6J genetic background. Heterozygous mice were successively backcrossed with C57BL/6J mice. F3 heterozygous mice were crossed to each other to obtain wild-type and PTPMEG-KO littermates. All behavioral and electrophysiological analyses were done in a blind manner to genotypes. Experiments with animals were carried out in accordance with the guidelines for animal use issued by the Committees of Animal Experiments of Institute of Medical Science, University of Tokyo, Kanazawa University, and Osaka University.

Preparation of cerebellar lysates and immunoblotting

Mice aged 4 days to 30 weeks were anaesthetized with diethyl either and their cerebella were lysed in a Tris/NP-40/EDTA buffer, and the lysates were subjected to immunoblotting as described (Hironaka *et al.*, 2000). A rabbit anti-PTPMEG antibody was described previously (Hironaka *et al.*, 2000). An anti-α-tubulin monoclonal antibody and an anti-Erk1 antibody were purchased from Sigma-Aldrich (St Louis, MO, USA) and Santa Cruz Biotechnology (Santa Cruz, CA, USA), respectively.

Histology

Mice aged 8 weeks were anaesthetized with diethyl ether and perfused with 4% paraformaldehyde/phosphate-buffered saline under deep ether anesthesia. Parasagittal cerebellar sections (20 μm thickness) were prepared by use of a cryostat, and stained with Cresyl violet or immunostained with an anti-calbindin antibody (SWANT, Bellinzona, Switzerland), followed by Alexa488-labeled goat anti-mouse IgG (Invitrogen, Carlsbad, CA, USA). The immunoreactive signals were obtained by a confocal microscopy (Olympus, Tokyo, Japan).

Animal behavioral analysis

Fixed-bar test

The fixed bar consisted of wood (either 6 mm or 20 mm in width, 80 cm in length, and 40 cm above the ground) was held horizontally on both ends. A mouse aged 8–10 weeks was placed on the bar, and the time was measured for which each mouse remained on the bar for a maximum of 60 s (Kadotani *et al.*, 1996). Data were statistically analysed by *t*-test. The difference was considered significant when P was less than 0.05.

Accelerated rotarod test

A mouse aged 8–9 weeks was placed on a drum (3 cm in diameter, polyvinyl chloride: Ohara, Tokyo, Japan) rotating at 4 r.p.m. at the beginning and, then, the rotation of the rotarod was accelerated from 4 to 40 r.p.m. over a 300-s period at a constant rate (Miyakawa *et al.*, 2001). The time was measured for which each mouse was able to maintain its balance on the rod. Mice were trained for two consecutive days, receiving four trials per day at intervals of 2 h between trials. Data were statistically analysed by a two-way repeated measures ANOVA. A *post hoc* comparison between the two genotypic groups for each trial was made with *t*-test (Granon *et al.*, 2003). The difference was considered significant when P was less than 0.05.

Classical eyeblink conditioning

Mice underwent surgery at the age of 8–11 weeks and conditioning experiments started at the age of 9–12 weeks. The surgical and conditioning procedures were basically the same as described previously (Kishimoto *et al.*, 2001c). Mice were anesthetized with ketamine (80 mg/kg, i.p.; Sankyo, Tokyo, Japan) and xylazine (20 mg/kg, i.p. Bayer, Tokyo, Japan). Four Teflon-coated stainless-steel wires (100 μm in diameter, A-M Systems, WA, USA) were implanted subcutaneously under the left eyelid. The two wires were used to record electromyograms (EMG) in the orbicuralis oculi muscle that detects an eyeblink, and the remaining two to deliver electrical shocks [unconditioned stimulus (US)]. A 100-ms periorbital shock (100 Hz square pulses) was used as the US, and a 450-ms tone (1.0 kHz, 80 dB) was used as the conditioned stimulus (CS). The US intensity was carefully determined as the minimal current amplitude required for eliciting an eyeblink response (about 0.2–0.3 mA) and constant unconditioned response (UR) amplitude (maximum EMG amplitude = 400%). In the delay eyeblink conditioning, the US overlapped the CS in time such that the two stimuli terminate simultaneously. The acquisition session consisted of 10 CS-only (every 10th trial) and 90 CS–US paired trials. The extinction session consisted of 100 CS-only trials. In pseudo-conditioning, the CS and US were randomly presented at an interstimulus interval ranging from 0 to 20 s. The spontaneous eyeblink frequency was measured by 100 'no stimulus' trials before the conditioning experiment began, and the startle response to a tone was measured during the initial 100 trials of the first session of the delay eyeblink conditioning. The UR amplitude was defined as the EMG amplitude at 50 ms after the US onset. All

© The Authors (2007). Journal Compilation © Federation of European Neuroscience Societies and Blackwell Publishing Ltd

experiments were performed during the light phase of a light : dark cycle in a container (10 cm in diameter) placed in a sound- and light-attenuating chamber. Data were statistically analysed by a two-way repeated measures ANOVA. A *post hoc* comparison between the two genotypic groups on each day was made with *t*-test. The difference was considered significant when *P* was less than 0.05 (Kishimoto *et al.*, 2001c, 2002; Granon *et al.*, 2003).

Electrophysiology

In the experiments in which the innervation patterns of CFs, the responses to paired pulses and the amplitude–intensity curve of the PF–PC synapses were examined, parasagittal cerebellar slices (250 μm thickness) were prepared from mice aged 4–9 weeks as described (Kano *et al.*, 1995; Kurihara *et al.*, 1997; Hashimoto *et al.*, 2001). The animals were anaesthetized with CO_2, and whole-cell recordings were made from visually identified PCs using an upright microscope (Olympus BX51WI) at 31 °C. Resistances of patch pipettes were 3–6 MΩ when filled with an intracellular solution composed of (in mM): CsCl, 60; Cs D-gluconate, 10; TEA-Cl, 20; BAPTA, 20; $MgCl_2$, 4; ATP, 4; GTP, 0.4; HEPES, 30 (pH 7.3). The pipette access resistance was compensated by 70–80%. The composition of standard bathing solution was (in mM): NaCl, 125; KCl, 2.5; $CaCl_2$, 2; $MgSO_4$, 1; NaH_2PO_4, 1.25; $NaHCO_3$, 26; glucose, 20; bubbled continuously with a mixture of 95% O_2 and 5% CO_2 (Hashimoto *et al.*, 2001). Bicuculline (10 μM) was always added to block inhibitory synaptic transmission mediated by γ-aminobutyric acid $(GABA)_A$ receptors. Excitatory postsynaptic currents (EPSCs) were recorded with an Axopatch 1D amplifier (Axon Instruments, Union City, CA, USA). The signals were filtered at 2 kHz and digitized at 20 kHz. On-line data acquisition and off-line data analysis were performed using PULSE software (HEKA, Lambrecht, Pfalz, Germany). Stimulation pipettes (5–10 μm in tip diameter) were filled with the standard saline and used to apply square pulses for focal stimulation (duration, 0.1 ms; amplitude, 0–90 V). CFs were stimulated in the granule cell layer 50–100 μm away from the PC soma. PFs were stimulated in the molecular layer.

In the experiments in which cerebellar LTD was examined, parasagittal cerebellar slices (250 μm thickness) were prepared from mice aged 8 weeks (anaesthetized with diethyl ether) and recorded basically as described (Namiki *et al.*, 2005; Kakizawa *et al.*, 2007). Resistances of patch pipettes were 1.8–3 MΩ when filled with an intracellular solution composed of (in mM): CsCl, 60; Cs D-gluconate, 40; TEA-Cl, 20; EGTA, 1; $MgCl_2$, 4; ATP, 4; GTP, 0.4; HEPES, 30 (pH 7.3). To monitor the amplitude of PF-mediated EPSCs (PF-EPSCs), test pulses were applied to PFs at 0.1 Hz, except for the period of conjunctive stimulation. The membrane potentials were held at −90 to −80 mV, after the compensation of liquid junction potential. The intensity of the stimulus was adjusted to evoke PF-EPSCs whose initial amplitudes were within the range between 100 and 200 pA. After the stable initial recording for at least 10 min, LTD was induced by the conjunctive stimulus, which was composed of 300 single PF stimuli in conjunction with a depolarizing pulse (for 50 ms from a holding potential of −90 or −80 mV to 0 mV) repeated at 1 Hz (Fujiwara *et al.*, 2007). The amplitude of PF-EPSC was normalized to the mean initial value recorded for 10 min before the conjunctive stimulus. Series resistance and membrane resistance were monitored throughout the experiments, and the data were discarded when either of these parameters changed by more than 10%. The data were also discarded when the slope of the baseline of PF-EPSC amplitudes during the initial recording for 10 min was larger than 2% (> 0.2% per min) or when the amplitude did not become stable within 30 min after the onset of whole-cell configuration (Namiki *et al.*, 2005; Kakizawa *et al.*, 2007).

Results

Generation of PTPMEG-KO mice

A targeting vector was constructed with a Tau-LacZ cassette inserted into the initiation codon of the PTPMEG open-reading frame (Fig. 1A). Targeted embryonic stem cells were selected, and correct integration of the targeting vector was confirmed by Southern blotting with PTPMEG- (Fig. 1B) and neomycin-resistance gene-specific probes (data not shown). The absence of PTPMEG expression was verified by Northern analysis (data not shown) and immunoblotting (Fig. 1C). The amount of PTPMEG in cerebellar lysates increased during postnatal development and peaked at 3–4 weeks after birth (Fig. 1D). Mice of all three genotypes were obtained at the expected Mendelian frequencies. PTPMEG-KO mice were fertile, and could be maintained for at least 16 months. Because we found defects of cerebellar functions in PTPMEG-KO mice (see below), we carried out histological examination of the cerebellum. In Nissl-stained sections, the main lobulation, the trilaminar organization of the cerebellar cortex and the monolayer alignment of PCs were grossly maintained in PTPMEG-KO mice (Fig. 1E and F). In addition, the immunohistochemical analysis for calbindin, a marker protein of PCs, did not reveal obvious defects in the development of PCs in PTPMEG-KO mice (Fig. 1G). Therefore, although subtle alterations could not be excluded, the normal cerebellar development was grossly maintained in PTPMEG-KO mice.

Impaired performance of PTPMEG-KO mice in the accelerated rotarod test

To evaluate the ability of motor coordination, we first performed the fixed-bar test (Fig. 2A). Wild-type and PTPMEG-KO mice could walk smoothly and stay on the bar (20 mm in width) with no difference in the time for which the mice stayed on the bar (wild-type, 59.29 ± 0.71 s, $n = 7$; PTPMEG-KO, 59.63 ± 0.12 s, $n = 8$; mean ± SEM, $P = 0.6159$). Even when a narrower bar (6 mm in width) was used, there was no significant difference between wild-type and PTPMEG-KO mice (wild-type, 52.14 ± 4.34 s, $n = 7$; PTPMEG-KO, 49.25 ± 3.65 s, $n = 8$; mean ± SEM, $P = 0.6695$). To further evaluate motor coordination and learning of PTPMEG-KO mice, we used the accelerated rotarod test (Fig. 2B). Wild-type and PTPMEG-KO mice performed similarly on the first trial (wild-type, 44.72 ± 9.56 s, $n = 18$; PTPMEG-KO, 30.11 ± 4.81 s, $n = 18$; mean ± SEM, $P = 0.1811$), which is a parameter of motor coordination. These results, together with those of the fixed-bar test, suggest that motor coordination is normal in PTPMEG-KO mice, although subtle defects that might be found in a more difficult test could not be ruled out. During the subsequent training, the performance of PTPMEG-KO mice to balance on the rod was significantly poorer than that of wild-type mice (genotype: $F_{1,34} = 15.57$, $P = 0.0037$; trial and genotype interaction: $F_{7,238} = 2.995$, $P = 0.005$). These data suggest that PTPMEG is required for the learning of motor skills (Nolan *et al.*, 2003).

Impaired memory formation in the cerebellum-dependent delay eyeblink conditioning in PTPMEG-KO mice

Next, we asked whether PTPMEG is involved in the delay eyeblink conditioning, which is one of the most extensively studied forms of cerebellum-dependent motor learning (Thompson & Kim, 1996; Thompson *et al.*, 1997). It has been shown that the delay eyeblink conditioning, in which the CS and US are given co-terminously to

© The Authors (2007). Journal Compilation © Federation of European Neuroscience Societies and Blackwell Publishing Ltd

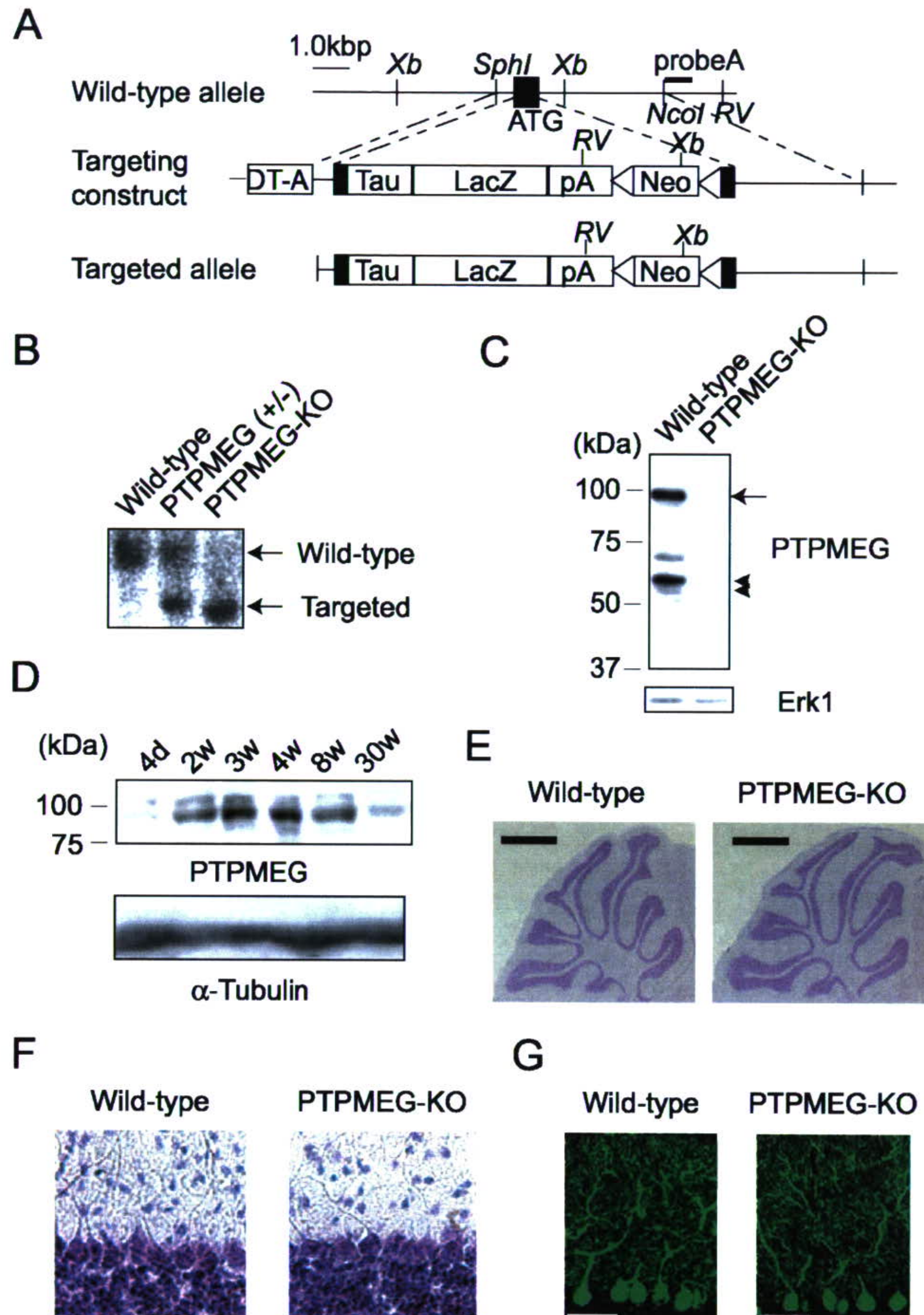

FIG. 1. Generation of PTPMEG-KO mice. (A) The restriction map of the PTPMEG genomic locus (top), targeting vector (middle) and targeted locus after homologous recombination (bottom). RV, EcoRV; Xb, XbaI. (B) Southern blot analysis. EcoRV-digested mouse tail DNAs were hybridized with probe A. A 20-kbp band and a 10.4-kbp band corresponding to wild-type and targeted alleles, respectively, were confirmed. (C) Western blot analysis. Cerebella of 8-week-old mice were lysed in a buffer containing NP-40, and the lysates were blotted with anti-PTPMEG (top) and anti-Erk1 (bottom) antibodies. The full-length (arrow) and truncated (arrowheads) products of PTPMEG are indicated, which are missing in the lysates of PTPMEG-knockout (KO) mice. (D) A temporal expression profile of PTPMEG. Cerebellar lysates from wild-type mice of the indicated ages were blotted with an anti-PTPMEG antibody (top) and an anti-α-tubulin monoclonal antibody (bottom) as a loading control. 4d, postnatal day 4; 2–30w, postnatal weeks 2–30. (E) Nissl-staining of parasagittal cerebellar sections from wild-type (left) and PTPMEG-KO (right) mice. Scale bar: 1 mm. (F) Magnified views of Nissl-stained sections. (G) Anti-calbindin immunostaining of parasagittal cerebellar sections. Scale bar: 50 μm.

mice, is cerebellum dependent (McCormick & Thompson, 1984; Chen *et al.*, 1996; Thompson *et al.*, 1997). In this paradigm, a 100-ms periorbital shock was used as the US and a 450-ms tone was used as the CS (Fig. 3B upper inset). Wild-type mice acquired the conditioned response (CR) more rapidly than PTPMEG-KO mice (Fig. 3A top). There was a significant difference between these genotypic groups (genotype: $F_{1,36} = 2.95$, $P = 0.49$; session and genotype interaction: $F_{6,216} = 4.46$, $P = 0.00028$). The deficit of CR acquisition at the early stage was more evident when analysing every 10-trial block of the daily acquisition session (Fig. 3A bottom). The sustained level of CR percentage (CR%) on Day 7 was similar between the two genotypic groups (Fig. 3A top). Consistently, the

© The Authors (2007). Journal Compilation © Federation of European Neuroscience Societies and Blackwell Publishing Ltd

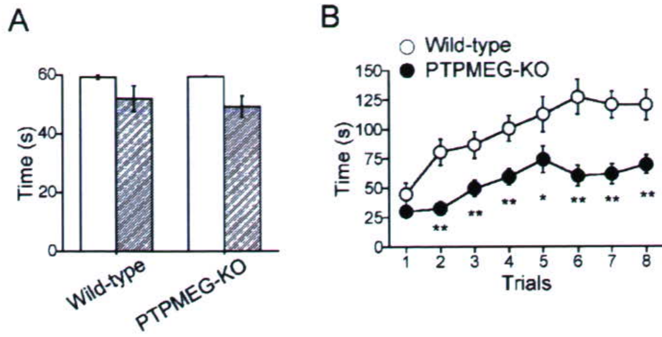

FIG. 2. Impaired performance of PTPMEG-knockout (KO) mice in the accelerated rotarod test. (A) Fixed-bar test. The time for which each mouse remained on the bar of either 20 mm (open columns) or 6 mm (hatched columns) in width was measured for a maximum of 60 s (wild-type, $n = 7$; PTPMEG-KO, $n = 8$). The data are expressed as the mean ± SEM. (B) Accelerated rotarod test. The rotation of the rod was accelerated from 4 to 40 r.p.m. over a 300-s period. A maximum retention time of 300 s was allowed for each mouse per trial. Wild-type mice (open circles, $n = 18$); PTPMEG-KO mice (closed circles, $n = 18$). The data are expressed as the mean ± SEM. $*P < 0.05$, $**P < 0.01$ (t-test).

averaged EMG amplitude for PTPMEG-KO mice was lower than that for the wild-type on Day 3, but not on Day 7 (Fig. 3B). As for the extinction of the learning, PTPMEG-KO mice showed no significant impairment at the whole extinction phase (Fig. 3A top; genotype: $F_{1,33} = 1.32$, $P = 0.26$; session and genotype interaction: $F_{3,99} = 1.53$, $P = 0.21$). These results demonstrated that PTPMEG was critical for rapid memory formation in the delay eyeblink conditioning.

No sensory deficit and the normal non-associative conditioning in PTPMEG-KO mice

There was no significant difference between wild-type and PTPMEG-KO mice in the UR amplitude in the delay eyeblink conditioning (Fig. 4A; genotype: $F_{1,33} = 0.15$, $P = 0.71$; session and genotype interaction: $F_{6,198} = 0.031$, $P = 0.99$). Furthermore, a startle response to the tone was comparable (wild-type, 2.09 ± 0.46%; PTPMEG-KO, 2.51 ± 0.53%, mean ± SEM). Next, to check a non-associative learning component, we tested the pseudo-conditioning with pseudo-randomized presentations of the CS and US (Fig. 4B). There was no significant difference between the two genotypic groups (genotype: $F_{1,8} = 0.004$, $P = 0.949$; session and genotype interaction: $F_{6,48} = 0.547$, $P = 0.769$). These results indicate that sensitivity to the CS and US, and performance of the eyeblink reflex are intact in PTPMEG-KO mice. Therefore, we concluded that the observed defects in motor learning were not likely due to deficits in the sensory perception or responses to the sensory stimuli.

Normal excitatory synaptic transmission in PCs of PTPMEG-KO mice

To investigate the abnormalities in cerebellar synaptic properties of PTPMEG-KO mice, we conducted whole-cell recordings of visually identified PCs in cerebellar slices and recorded EPSCs by stimulating CFs and PFs. We first tested whether multiple CF innervation persisted in PTPMEG-KO mice. Individual PCs are innervated by multiple CFs during early postnatal development, but supernumerary CFs are subsequently pruned, and most PCs are innervated by a single CF by 3 weeks after birth (Hashimoto & Kano, 2005). Several strains of mice with abnormal retention of multiple CF

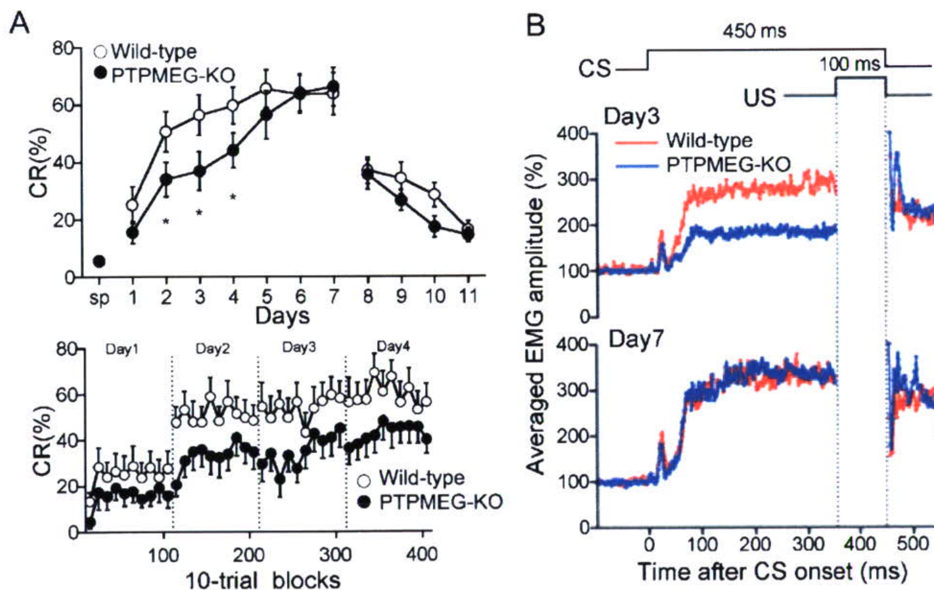

FIG. 3. Impaired acquisition of the delay eyeblink conditioning in PTPMEG-knockout (KO) mice. (A) Development of the conditioned response (CR)% during the delay eyeblink conditioning in wild-type (open circles, $n = 16$) and PTPMEG-KO (closed circles, $n = 22$) mice. (top) The averaged CR% on each day is plotted at the acquisition phase from Day 1 to Day 7. Daily sessions consisted of 10 blocks of trials. Each block consisted of nine conditioned stimulus (CS)–unconditioned stimulus (US) paired trials and one CS-only trial. At the following 4-day extinction phase, 100 CS-only presentations were given daily. 'sp' represents spontaneous eyeblink responses. The data are expressed as the mean ± SEM. $*P < 0.05$ (t-test). (bottom) When the CR% was plotted by 10-trial blocks, retarded acquisition of the CR in PTPMEG-KO mice was more clearly observed. The data are expressed as the mean ± SEM. (B) The averaged electromyogram (EMG) amplitudes of eyeblink responses for wild-type (red trace) and PTPMEG-KO (blue trace) mice on Day 3 (top) and Day 7 (bottom). Although PTPMEG-KO mice caught up with wild-type mice at the end of the training session (bottom), the top panel clearly indicates that PTPMEG-KO mice exhibited a significantly lower EMG response to the tone CS at the early stage of the conditioning training.

© The Authors (2007). Journal Compilation © Federation of European Neuroscience Societies and Blackwell Publishing Ltd

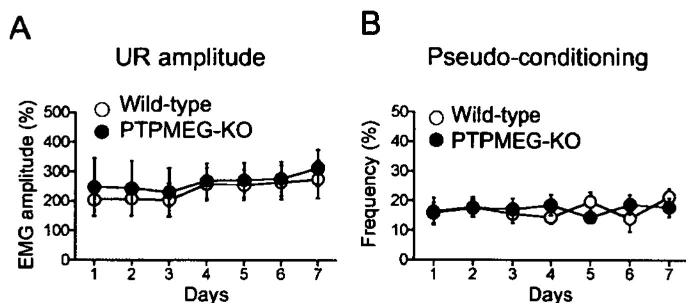

FIG. 4. Normal sensitivity to sensory stimuli and intact pseudo-conditioning in PTPMEG-knockout (KO) mice. (A) The averaged unconditioned response (UR) amplitudes for wild-type ($n = 16$) and PTPMEG-KO ($n = 22$) mice during the delay eyeblink conditioning (Fig. 3). In both genotypic groups, the UR amplitudes were nearly constant throughout the 7-day acquisition phase. No difference was observed between wild-type and PTPMEG-KO mice. (B) The pseudo-conditioning in wild-type ($n = 7$) and PTPMEG-KO ($n = 7$) mice. The CS and US were randomly presented at an interstimulus interval ranging from 0 to 20 s (10 s average). The eyelid response to the CS did not increase in either wild-type or PTPMEG-KO mice. The data are expressed as the mean ± SEM. EMG, electromyogram.

innervation, such as PKCγ- and GluRδ2-KO mice, show impaired motor coordination (Kano *et al.*, 1995; Hashimoto *et al.*, 2001). As shown in Fig. 5A, the distribution of PCs in terms of the number of CF-mediated EPSC (CF-EPSC) steps was not significantly different between wild-type and PTPMEG-KO mice ($P = 0.943$, χ^2-test), which is consistent with the normal motor coordination observed in PTPMEG-KO mice. We also examined the kinetics and short-term plasticity of EPSCs elicited by stimulation of mono-innervating CFs. The 10–90% rise times, decay time constants and chord conductance calculated between the holding potential of −10 mV and +50 mV were similar between wild-type and PTPMEG-KO mice (data not shown). The paired-pulse depression of CF-EPSCs was also similar between wild-type and PTPMEG-KO mice (Fig. 5B). Therefore, it is likely that the CF-mediated calcium entry, which is critical for the induction of LTD at PF–PC synapses (Sakurai, 1990; Konnerth *et al.*, 1992), would be normal in PTPMEG-KO PCs. Next, we examined whether the PF synaptic transmission was affected in PTPMEG-KO mice. We stimulated PFs at different intensities, and amplitudes of PF-EPSCs were plotted as a function of stimulus intensities. As shown in Fig. 6A, the slopes of the amplitude–intensity curves were similar between wild-type and PTPMEG-KO PCs ($P > 0.05$, *t*-test). Furthermore, the 10–90% rise times and decay time constants in PF-EPSCs and the paired-pulse facilitation of PF-EPSCs were indistinguishable between wild-type and PTPMEG-KO mice (Fig. 6B). These results suggest that the developmental elimination of surplus CFs and the physiological properties of excitatory synaptic inputs to PCs are basically normal in PTPMEG-KO mice.

Impairment of cerebellar LTD in PTPMEG-KO mice

We next examined whether the lack of PTPMEG affected cerebellar LTD at PF–PC synapses. After stable recordings of PF-EPSCs for 10 min, LTD was induced by a conventional conjunction protocol, which consisted of 300 single PF stimuli in conjunction with a depolarizing pulse repeated at 1 Hz. In wild-type mice, LTD was readily induced by the conjunctive stimulation (Fig. 7A). At 21–30 min after the conditioning, the mean amplitude of EPSCs elicited by PF stimulation was reduced to 61.9 ± 2.1% (mean ± SEM) of the control value measured prior to the conjunctive stimulation (Fig. 7B). The same conjunctive stimulation also induced LTD in PTPMEG-KO mice. However, the mean value of the EPSC amplitude at 21–30 min after the conditioning (76.8 ± 2.4%) was significantly higher ($P = 0.00038$, *t*-test) than the wild-type value (Fig. 7A and B). Therefore, cerebellar LTD was present but impaired in PTPMEG-KO mice, suggesting that PTPMEG-mediated tyrosine dephosphorylation events have a modulatory role in cerebellar LTD.

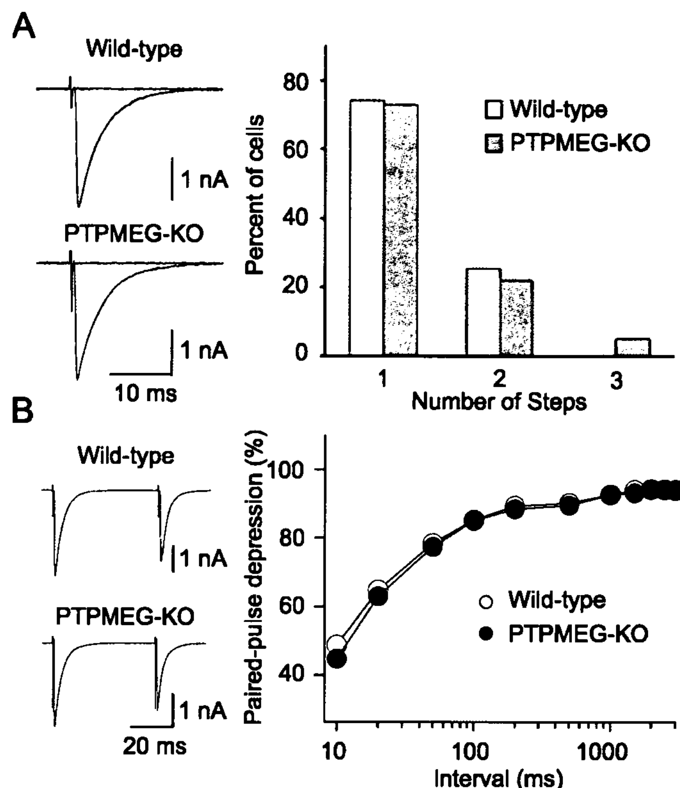

FIG. 5. Normal excitatory synaptic transmission in the CF–PC synapses of PTPMEG-knockout (KO) mice. (A) Innervation patterns of CFs. (left) Representative traces of CF-EPSCs recorded from wild-type (top) and PTPMEG-KO (bottom) PCs. CFs were stimulated in the granule cell layer at 0.2 Hz. Four traces evoked with the threshold stimulus intensity are superimposed. The holding potential was −20 mV. (right) Summary histograms showing the number of discrete steps in CF-EPSCs of wild-type (open columns, $n = 39$) and PTPMEG-KO (hatched columns, $n = 59$) PCs. The percentage of PCs with more than one discrete CF-EPSC step was similar between the two genotypic groups ($P = 0.943$, χ^2 test for independent samples). (B) Short-term synaptic plasticity of CF-EPSCs. (left) Representative traces of CF-EPSCs evoked by paired pulses at an interpulse interval of 50 ms. Three traces were averaged. (right) Summary graph showing paired-pulse depression of CF-EPSCs in wild-type (open circles, $n = 11$) and PTPMEG-KO (closed circles, $n = 14$) PCs. The amplitude of the second response is expressed as a percentage of the first response (mean ± SEM) and is plotted as a function of interpulse intervals. Stimulus pairs were applied at 0.2 Hz. The holding potential was −20 mV.

Discussion

In this study, we demonstrated that PTPMEG-KO mice showed impairment in motor learning and cerebellar LTD. To our knowledge, mice devoid of a PTK or a PTP that show defects in cerebellar LTD and motor learning have not been reported.

PTPMEG belongs to a subfamily of cytoplasmic PTPs that contains FERM and catalytic PTP domains (Alonso *et al.*, 2004). This PTP

© The Authors (2007). Journal Compilation © Federation of European Neuroscience Societies and Blackwell Publishing Ltd

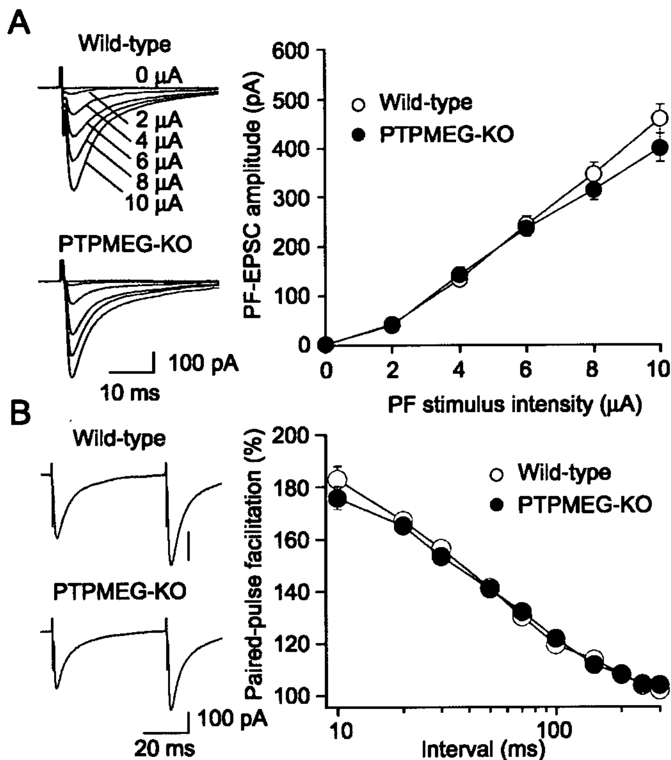

FIG. 6. Normal excitatory synaptic transmission in the parallel fiber (PF)–PC synapses of PTPMEG-knockout (KO) mice. (A) Input–output relationship of the PF-excitatory postsynaptic currents (EPSCs). (left) Representative traces of PF-EPSCs with increasing stimulus intensities (0–10 μA) recorded from wild-type (top) and PTPMEG-KO (bottom) PCs. (right) Amplitudes of PF-EPSCs plotted as a function of stimulus intensities in the wild-type (open circles, $n = 26$) and PTPMEG-KO (closed circles, $n = 19$) PCs. Each point represents the mean ± SEM. There was no significant difference between wild-type and PTPMEG-KO mice ($P > 0.05$, t-test). (B) Short-term synaptic plasticity of PF-EPSCs. (left) Representative traces of PF-EPSCs evoked by paired pulses at an interpulse interval of 50 ms. Ten traces were averaged. (right) Summary graph showing paired-pulse facilitation of PF-EPSCs in wild-type (open circles, $n = 17$) and PTPMEG-KO (closed circles, $n = 20$) PCs. The amplitude of the second response is expressed as a percentage of the first response (mean ± SEM) and is plotted as a function of interpulse intervals. There was no significant difference between wild-type and PTPMEG-KO mice. Stimulus pairs were applied at 0.5 Hz. The holding potential was −80 mV.

family consists of PTPMEG, PTPH1/PTPN3, PTPD1/PTPN21, PTPD2/PTPN14 and PTP-BL/PTPN13. In addition, three PTPs of this family have one (PTPMEG and PTPH1) or five (PTP-BL) PDZ domains. PTPH1 is the closest homolog of PTPMEG (Yang & Tonks, 1991). Mice lacking PTP-BL phosphatase activity are mildly impaired in motor nerve repair after sciatic nerve lesions (Wansink *et al.*, 2004). Mice lacking PTPH1 phosphatase activity show normal signal transduction upon stimulation of T-cell antigen receptors (Bauler *et al.*, 2007). Physiological importance of this PTP family in the mammalian CNS had not been demonstrated.

Tyrosine phosphorylation/dephosphorylation is thought to be involved in the cerebellar development, including the layer formation, CF-PC synapse elimination and PC morphology (Howell *et al.*, 2000; Meathrel *et al.*, 2002; Kakizawa *et al.*, 2003; Tanaka *et al.*, 2003). Axons of cerebellar granule cells are disorganized and tangled in mice lacking PTPσ/PTPRS, a receptor-type PTP (Meathrel *et al.*, 2002). Signaling through PTPζ/RPTPβ/PTPRZ1 regulates the morphogenesis of PC dendrites (Tanaka *et al.*, 2003). In addition, *Drosophila* PTPMEG is involved in the proper establishment and maintenance of axon projections in the central brain (Whited *et al.*, 2007). The expression level of PTPMEG was low during the cerebellar development, and the normal cerebellar development of PTPMEG-KO mice was grossly maintained, although subtle alterations could not be excluded. Consistently, the developmental elimination of surplus CFs of PCs normally occurred in PTPMEG-KO mice (Fig. 5A). However, other FERM-containing PTPs, especially PTPH1 that is reported to be expressed in the cerebellum (Sahin *et al.*, 1995), may compensate for the lack of PTPMEG in the mutant mice. Mice lacking both PTPMEG and PTPH1 might reveal roles of these PTPs in the cerebellar development.

We found mild, but significant, impairment in both acquisition of the cerebellum-dependent delay eyeblink conditioning and cerebellar LTD at PF–PC synapses in PTPMEG-KO mice. Cerebellar LTD was present, but attenuated, in these mice (Fig. 7). The delay eyeblink conditioning was also impaired in these mice during the early stage of acquisition (Fig. 3). These results suggest that PTPMEG-regulated tyrosine dephosphorylation events are not indispensable for, but modulate, cerebellar LTD and motor learning. Alternatively, other PTPs such as PTPH1 may also contribute to cerebellar synaptic plasticity. It would be obviously important to further clarify roles of PTPMEG and the related PTPs in the adult cerebellum.

Cellular mechanisms underlying defects in motor learning in PTPMEG-KO mice

Many previous studies strongly suggest that LTD at PF–PC synapses underlies motor learning in the cerebellum (Ito, 2001). Several mutant mice that have defects in LTD show impairment in the delay eyeblink conditioning. These mouse models include mice lacking mGluR1 (Aiba *et al.*, 1994; Kishimoto *et al.*, 2002), GluRδ2 (Kishimoto *et al.*, 2001c), phospholipase Cβ4 (Kishimoto *et al.*, 2001a; Miyata *et al.*, 2001) and CB1 cannabinoid receptors (Safo & Regehr, 2005; Kishimoto & Kano, 2006). In these four mutant mice, the defects are more severe than those in PTPMEG-KO mice: cerebellar LTD is deficient, and the sustained levels of CR% in the delay eyeblink conditioning are severely impaired. In addition, both LTD and delay eyeblink conditioning are restored in mGluR1-rescue mice in which mGluR1α is expressed only in PCs in mGluR1-KO mice by using a PC-specific promoter (Ichise *et al.*, 2000; Kishimoto *et al.*, 2002). These findings are consistent with the notion that cerebellar LTD is a cellular substrate of the delay eyeblink conditioning. Therefore, it is likely that impairment in LTD is a cause of impaired acquisition of the delay eyeblink conditioning in PTPMEG-KO mice. To support this idea, the sustained level of CR% was comparable between wild-type and PTPMEG-KO mice, which might be explained by impaired but still significant cerebellar LTD in the absence of PTPMEG. However, PTPMEG is expressed not only in PCs, but also in the thalamus, cortex and hippocampus (Hironaka *et al.*, 2000). Therefore, we could not exclude the possibility that PTPMEG expressed in neurons other than PCs is critical for the motor-memory formation. The phenotype of PTPMEG-KO mice in the delay eyeblink conditioning bears a closer resemblance to that of GluRε1/NR2A-KO mice (Kishimoto *et al.*, 1997, 2001b), which exhibit impaired long-term potentiation (LTP) in the hippocampal CA1 region (Sakimura *et al.*, 1995). At the early stage of the delay conditioning training, GluRε1-KO mice also exhibit lower CR% and EMG amplitude, but they catch up with wild-type mice in the CR% by the end of the conditioning training (Kishimoto *et al.*, 1997, 2001c). Taking account of the fact that PTPMEG interacts not only with GluRδ2 but also with GluRε1

© The Authors (2007). Journal Compilation © Federation of European Neuroscience Societies and Blackwell Publishing Ltd

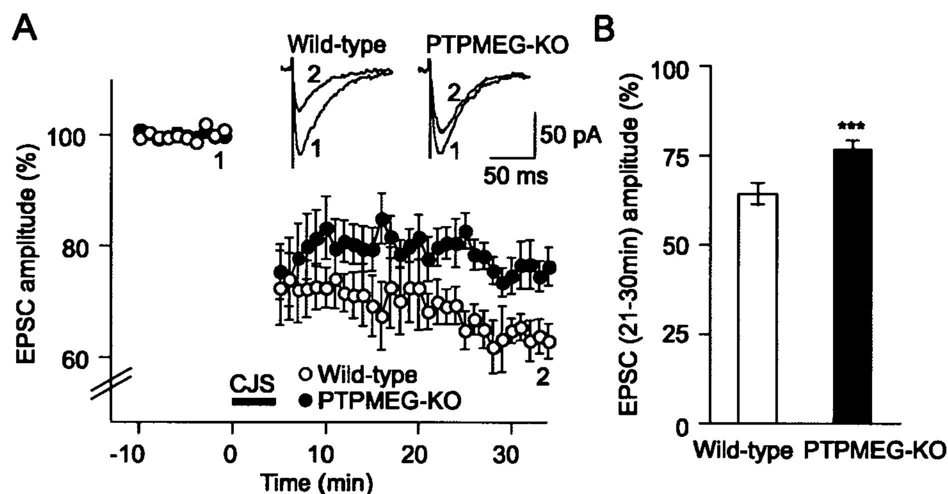

FIG. 7. Impaired cerebellar LTD in PTPMEG-knockout (KO) mice. (A) Cerebellar LTD. Summary of changes in the amplitude of PF-excitatory postsynaptic currents (EPSCs) before and after the conjunctive stimulus (CJS, solid bar) in wild-type (open circles, $n = 6$) and PTPMEG-KO (closed circles, $n = 8$) mice. The amplitude was normalized to the mean initial value recorded for 10 min before the CJS. Insets show sample traces of PF-EPSCs recorded just before (1) and 30 min after (2) the CJS. The data are expressed as the mean ± SEM. (B) The mean amplitude of PF-EPSCs at 21–30 min after the CJS in (A) in wild-type (open column, $n = 6$) and PTPMEG-KO mice (closed column, $n = 8$). The data are expressed as the mean ± SEM. $^{***}P = 0.00038$ (t-test).

(Hironaka *et al.*, 2000), PTPMEG expressed in other brain regions such as the hippocampus might be involved in the rapid memory formation in the eyeblink conditioning.

Molecular mechanisms of the regulation of cerebellar functions by PTPMEG

Recent studies have identified several PTKs, PTPs and their substrates that are critical for hippocampal synaptic plasticity and hippocampus-dependent learning. For example, Fyn-KO and EphB2-KO mice show impairment in hippocampal functions (Grant *et al.*, 1992; Grunwald *et al.*, 2001). PTPα/PTPRA-KO mice show impaired LTP in the hippocampal CA1 region and poor performance in the radial arm-maze and water-maze tests (Petrone *et al.*, 2003). PTPδ/PTPRD-KO mice also show learning impairment in the water-maze, reinforced T-maze and radial arm-maze tests with enhanced LTP and paired-pulse facilitation in the hippocampal CA1 region (Uetani *et al.*, 2000). PTPRZ1-KO mice show age-dependent enhancement of hippocampal LTP and impairment in the water-maze test (Niisato *et al.*, 2005). The *N*-methyl-D-aspartate (NMDA)-type glutamate receptors (NMDARs), which play pivotal roles in hippocampus-dependent spatial learning and LTP in hippocampal CA1 neurons, are regulated by their tyrosine phosphorylation status (Salter & Kalia, 2004). Currents through NMDARs are potentiated by Src-family PTKs. Tyrosine dephosphorylation of NMDARs is implicated in receptor internalization (Snyder *et al.*, 2005). In contrast, tyrosine phosphorylation of GluR2 results in its endocytosis, leading to the reduction of AMPAR-mediated currents (Ahmadian *et al.*, 2004). However, little is known about PTKs and their substrates in cerebellar synaptic plasticity. Functional NMDARs are not expressed in PCs, and the level of GluR2 tyrosine phosphorylation in the cerebellum is low (Hayashi & Huganir, 2004). Identification of the substrates of PTPMEG would clarify the mechanisms of cerebellar LTD and motor learning. Our preliminary data showed that tyrosine phosphorylation of a protein with an approximate mass of 73 kDa was elevated in the cerebellum of 8-week-old PTPMEG-KO mice (data not shown). Further characterization of the 73 kDa protein as well as other possible targets would be important.

Regulation of PTPMEG in the cerebellum is currently elusive. GluRδ2 can regulate PTPMEG, as PTPMEG binds to GluRδ2 through its PDZ domain (Hironaka *et al.*, 2000). However, GluRδ2-KO mice have severe abnormalities not only in the cerebellar LTD and delay eyeblink conditioning, but also in the PF–PC synapse formation and CF innervation pattern (Kurihara *et al.*, 1997; Hashimoto *et al.*, 2001; Ichikawa *et al.*, 2002), whereas PTPMEG-KO mice exhibited a normal CF innervation pattern (Fig. 5A). In addition, the PF–PC synapse formation would also be normal in PTPMEG-KO mice because defects in PF innervation lead to abnormal CF innervation (Hashimoto *et al.*, 2001). Indeed, PTPMEG-KO mice showed normal responses of PCs to PF stimulation (Fig. 6A). Thus, PTPMEG is not likely to be involved in the signaling cascade controlling the excitatory synapse formation on PCs. On the other hand, because the magnitude of LTD, which is completely absent in GluRδ2-KO mice, was attenuated in PTPMEG-KO mice (Fig. 7), regulation of LTD by GluRδ2 may involve PTPMEG at least partly. GluRδ2 is localized to the postsynaptic density of PF–PC synapses, which are formed on spines of distal PC dendrites (Landsend *et al.*, 1997). PTPMEG is also found in the postsynaptic density of the cerebellum (Hironaka *et al.*, 2000). Moreover, PDZ proteins that bind to the carboxyl-terminus of GluRδ2 are crucial for conveying signals necessary for the induction of LTD in cerebellar slices (Kohda *et al.*, 2007), although another report shows that the membrane-proximal but not PDZ-binding sequence in the cytoplasmic region of GluRδ2 is crucial for cerebellar LTD in cultured PCs (Yawata *et al.*, 2006). Therefore, GluRδ2 may partly function as a scaffold protein for intracellular signaling molecules such as PTPMEG (Yuzaki, 2004). In addition, it is also possible that mGluR1 regulates PTPMEG, because two PTP inhibitors, orthovanadate and phenylarsine oxide, block hippocampal LTD induced by the type I mGluR agonist (*RS*)-3,5-dihydroxyphenylglycine stimulation (Moult *et al.*, 2006). Moreover, the elevation of intracellular Ca^{2+}, which is essential for cerebellar LTD (Sakurai, 1990; Konnerth *et al.*, 1992), may also regulate PTPMEG. Calpain, a Ca^{2+}-dependent protease, is involved in the Ca^{2+}-dependent signaling pathway in PCs (Hirai, 2001). Interestingly, the phosphatase activity of PTPMEG increases when it is cleaved by calpain (Gu & Majerus, 1996), raising the possibility that PTPMEG is activated upon the

© The Authors (2007). Journal Compilation © Federation of European Neuroscience Societies and Blackwell Publishing Ltd

induction of cerebellar LTD. The subcellular localization and activity of PTPMEG during cerebellar LTD would be critical issues to be addressed.

Acknowledgements

We thank Drs K. Hironaka and J. Goto for their help on the generation and analysis of PTPMEG-KO mice. This research was supported in part by Grants-in-Aids for Scientific Research on Priority Areas and National Project on Protein Structural and Functional Analyses from Ministry of Education, Culture, Sports, Science and Technology of Japan.

Abbreviations

AMPAR, α-amino-3-hydroxy-5-methyl-4-isoxazolepropionic acid type receptor; CF, climbing fiber; CR, conditioned response; CS, conditioned stimulus; EMG, electromyogram; EPSC, excitatory postsynaptic current; GluR, glutamate receptor; KO, knockout; LTD, long-term depression; LTP, long-term potentiation; mGluR, metabotropic glutamate receptor; NMDA, *N*-methyl-D-aspartate; PC, Purkinje cell; PDZ, postsynaptic density-95/discs-large/ZO-1; PF, parallel fiber; PKC, protein kinase C; PTK, protein-tyrosine kinase; PTP, protein-tyrosine phosphatase; UR, unconditioned response; US, unconditioned stimulus.

References

Ahmadian, G., Ju, W., Liu, L., Wyszynski, M., Lee, S.H., Dunah, A.W., Taghibiglou, C., Wang, Y., Lu, J., Wong, T.P., Sheng, M. & Wang, Y.T. (2004) Tyrosine phosphorylation of GluR2 is required for insulin-stimulated AMPA receptor endocytosis and LTD. *EMBO J.*, **23**, 1040–1050.

Aiba, A., Kano, M., Chen, C., Stanton, M.E., Fox, G.D., Herrup, K., Zwingman, T.A. & Tonegawa, S. (1994) Deficient cerebellar long-term depression and impaired motor learning in mGluR1 mutant mice. *Cell*, **79**, 377–388.

Alonso, A., Sasin, J., Bottini, N., Friedberg, I., Friedberg, I., Osterman, A., Godzik, A., Hunter, T., Dixon, J. & Mustelin, T. (2004) Protein tyrosine phosphatases in the human genome. *Cell*, **117**, 699–711.

Bauler, T.J., Hughes, E.D., Arimura, Y., Mustelin, T., Saunders, T.L. & King, P.D. (2007) Normal TCR signal transduction in mice that lack catalytically active PTPN3 protein tyrosine phosphatase. *J. Immunol.*, **178**, 3680–3687.

Boxall, A.R., Lancaster, B. & Garthwaite, J. (1996) Tyrosine kinase is required for long-term depression in the cerebellum. *Neuron*, **16**, 805–813.

Boyden, E.S., Katoh, A. & Raymond, J.L. (2004) Cerebellum-dependent learning: the role of multiple plasticity mechanisms. *Annu. Rev. Neurosci.*, **27**, 581–609.

Callahan, C.A. & Thomas, J.B. (1994) Tau-β-galactosidase, an axon-targeted fusion protein. *Proc. Natl Acad. Sci. USA*, **91**, 5972–5976.

Castro-Alamancos, M.A. & Torres-Aleman, I. (1994) Learning of the conditioned eye-blink response is impaired by an antisense insulin-like growth factor I oligonucleotide. *Proc. Natl Acad. Sci. USA*, **91**, 10203–10207.

Chen, L., Bao, S., Lockard, J.M., Kim, J.K. & Thompson, R.F. (1996) Impaired classical eyeblink conditioning in cerebellar-lesioned and Purkinje cell degeneration (pcd) mutant mice. *J. Neurosci.*, **16**, 2829–2838.

Chung, H.J., Steinberg, J.P., Huganir, R.L. & Linden, D.J. (2003) Requirement of AMPA receptor GluR2 phosphorylation for cerebellar long-term depression. *Science*, **300**, 1751–1755.

Fujiwara, A., Kakizawa, S. & Iino, M. (2007) Induction of cerebellar long-term depression requires activation of calcineurin in Purkinje cells. *Neuropharmacology*, **52**, 1663–1670.

Granon, S., Faure, P. & Changeux, J.P. (2003) Executive and social behaviors under nicotinic receptor regulation. *Proc. Natl Acad. Sci. USA*, **100**, 9596–9601.

Grant, S.G., O'Dell, T.J., Karl, K.A., Stein, P.L., Soriano, P. & Kandel, E.R. (1992) Impaired long-term potentiation, spatial learning, and hippocampal development in fyn mutant mice. *Science*, **258**, 1903–1910.

Grunwald, I.C., Korte, M., Wolfer, D., Wilkinson, G.A., Unsicker, K., Lipp, H.P., Bonhoeffer, T. & Klein, R. (2001) Kinase-independent requirement of EphB2 receptors in hippocampal synaptic plasticity. *Neuron*, **32**, 1027–1040.

Gu, M. & Majerus, P.W. (1996) The properties of the protein tyrosine phosphatase PTPMEG. *J. Biol. Chem.*, **271**, 27751–27759.

Gu, M., Meng, K. & Majerus, P.W. (1996) The effect of overexpression of the protein tyrosine phosphatase PTPMEG on cell growth and on colony formation in soft agar in COS-7 cells. *Proc. Natl Acad. Sci. USA*, **93**, 12980–12985.

Gu, M.X., York, J.D., Warshawsky, I. & Majerus, P.W. (1991) Identification, cloning, and expression of a cytosolic megakaryocyte protein-tyrosine-phosphatase with sequence homology to cytoskeletal protein 4.1. *Proc. Natl Acad. Sci. USA*, **88**, 5867–5871.

Hashimoto, K., Ichikawa, R., Takechi, H., Inoue, Y., Aiba, A., Sakimura, K., Mishina, M., Hashikawa, T., Konnerth, A., Watanabe, M. & Kano, M. (2001) Roles of glutamate receptor δ2 subunit (GluRδ2) and metabotropic glutamate receptor subtype 1 (mGluR1) in climbing fiber synapse elimination during postnatal cerebellar development. *J. Neurosci.*, **21**, 9701–9712.

Hashimoto, K. & Kano, M. (2005) Postnatal development and synapse elimination of climbing fiber to Purkinje cell projection in the cerebellum. *Neurosci. Res.*, **53**, 221–228.

Hayashi, T. & Huganir, R.L. (2004) Tyrosine phosphorylation and regulation of the AMPA receptor by SRC family tyrosine kinases. *J. Neurosci.*, **24**, 6152–6160.

Hirai, H. (2001) Ca^{2+}-dependent regulation of synaptic δ2 glutamate receptor density in cultured rat Purkinje neurons. *Eur. J. Neurosci.*, **14**, 73–82.

Hirai, H., Launey, T., Mikawa, S., Torashima, T., Yanagihara, D., Kasaura, T., Miyamoto, A. & Yuzaki, M. (2003) New role of δ2-glutamate receptors in AMPA receptor trafficking and cerebellar function. *Nat. Neurosci.*, **6**, 869–876.

Hironaka, K., Umemori, H., Tezuka, T., Mishina, M. & Yamamoto, T. (2000) The protein-tyrosine phosphatase PTPMEG interacts with glutamate receptor δ2 and ϵ subunits. *J. Biol. Chem.*, **275**, 16167–16173.

Howell, B.W., Herrick, T.M., Hildebrand, J.D., Zhang, Y. & Cooper, J.A. (2000) Dab1 tyrosine phosphorylation sites relay positional signals during mouse brain development. *Curr. Biol.*, **10**, 877–885.

Ichikawa, R., Miyazaki, T., Kano, M., Hashikawa, T., Tatsumi, H., Sakimura, K., Mishina, M., Inoue, Y. & Watanabe, M. (2002) Distal extension of climbing fiber territory and multiple innervation caused by aberrant wiring to adjacent spiny branchlets in cerebellar Purkinje cells lacking glutamate receptor δ2. *J. Neurosci.*, **22**, 8487–8503.

Ichise, T., Kano, M., Hashimoto, K., Yanagihara, D., Nakao, K., Shigemoto, R., Katsuki, M. & Aiba, A. (2000) mGluR1 in cerebellar Purkinje cells essential for long-term depression, synapse elimination, and motor coordination. *Science*, **288**, 1832–1835.

Ito, M. (2001) Cerebellar long-term depression: characterization, signal transduction, and functional roles. *Physiol. Rev.*, **81**, 1143–1195.

Ito, M. (2002) The molecular organization of cerebellar long-term depression. *Nat. Rev. Neurosci.*, **3**, 896–902.

Kadotani, H., Hirano, T., Masugi, M., Nakamura, K., Nakao, K., Katsuki, M. & Nakanishi, S. (1996) Motor discoordination results from combined gene disruption of the NMDA receptor NR2A and NR2C subunits, but not from single disruption of the NR2A or NR2C subunit. *J. Neurosci.*, **16**, 7859–7867.

Kakizawa, S., Kishimoto, Y., Hashimoto, K., Miyazaki, T., Furutani, K., Shimizu, H., Fukaya, M., Nishi, M., Sakagami, H., Ikeda, A., Kondo, H., Kano, M., Watanabe, M., Iino, M. & Takeshima, H. (2007) Junctophilin-mediated channel crosstalk essential for cerebellar synaptic plasticity. *EMBO J.*, **26**, 1924–1933.

Kakizawa, S., Yamada, K., Iino, M., Watanabe, M. & Kano, M. (2003) Effects of insulin-like growth factor I on climbing fibre synapse elimination during cerebellar development. *Eur. J. Neurosci.*, **17**, 545–554.

Kano, M., Hashimoto, K., Chen, C., Abeliovich, A., Aiba, A., Kurihara, H., Watanabe, M., Inoue, Y. & Tonegawa, S. (1995) Impaired synapse elimination during cerebellar development in PKCγ mutant mice. *Cell*, **83**, 1223–1231.

Kashiwabuchi, N., Ikeda, K., Araki, K., Hirano, T., Shibuki, K., Takayama, C., Inoue, Y., Kutsuwada, T., Yagi, T., Kang, Y., Aizawa, S. & Mishina, M. (1995) Impairment of motor coordination, Purkinje cell synapse formation, and cerebellar long-term depression in GluRδ2 mutant mice. *Cell*, **81**, 245–252.

Kishimoto, Y., Fujimichi, R., Araishi, K., Kawahara, S., Kano, M., Aiba, A. & Kirino, Y. (2002) mGluR1 in cerebellar Purkinje cells is required for normal association of temporally contiguous stimuli in classical conditioning. *Eur. J. Neurosci.*, **16**, 2416–2424.

Kishimoto, Y., Hirono, M., Sugiyama, T., Kawahara, S., Nakao, K., Kishio, M., Katsuki, M., Yoshioka, T. & Kirino, Y. (2001a) Impaired delay but normal trace eyeblink conditioning in PLCβ4 mutant mice. *Neuroreport*, **12**, 2919–2922.

© The Authors (2007). Journal Compilation © Federation of European Neuroscience Societies and Blackwell Publishing Ltd

Kishimoto, Y. & Kano, M. (2006) Endogenous cannabinoid signaling through the CB1 receptor is essential for cerebellum-dependent discrete motor learning. *J. Neurosci.*, **26**, 8829-8837.

Kishimoto, Y., Kawahara, S., Kirino, Y., Kadotani, H., Nakamura, Y., Ikeda, M. & Yoshioka, T. (1997) Conditioned eyeblink response is impaired in mutant mice lacking NMDA receptor subunit NR2A. *Neuroreport*, **8**, 3717–3721.

Kishimoto, Y., Kawahara, S., Mori, H., Mishina, M. & Kirino, Y. (2001b) Long-trace interval eyeblink conditioning is impaired in mutant mice lacking the NMDA receptor subunit ϵ1. *Eur. J. Neurosci.*, **13**, 1221–1227.

Kishimoto, Y., Kawahara, S., Suzuki, M., Mori, H., Mishina, M. & Kirino, Y. (2001c) Classical eyeblink conditioning in glutamate receptor subunit δ2 mutant mice is impaired in the delay paradigm but not in the trace paradigm. *Eur. J. Neurosci.*, **13**, 1249–1253.

Kohda, K., Kakegawa, W., Matsuda, S., Nakagami, R., Kakiya, N. & Yuzaki, M. (2007) The extreme C-terminus of GluRδ2 is essential for induction of long-term depression in cerebellar slices. *Eur. J. Neurosci.*, **25**, 1357–1362.

Konnerth, A., Dreessen, J. & Augustine, G.J. (1992) Brief dendritic calcium signals initiate long-lasting synaptic depression in cerebellar Purkinje cells. *Proc. Natl Acad. Sci. USA*, **89**, 7051–7055.

Kurihara, H., Hashimoto, K., Kano, M., Takayama, C., Sakimura, K., Mishina, M., Inoue, Y. & Watanabe, M. (1997) Impaired parallel fiber → Purkinje cell synapse stabilization during cerebellar development of mutant mice lacking the glutamate receptor δ2 subunit. *J. Neurosci.*, **17**, 9613–9623.

Landsend, A.S., Amiry-Moghaddam, M., Matsubara, A., Bergersen, L., Usami, S., Wenthold, R.J. & Ottersen, O.P. (1997) Differential localization of δ glutamate receptors in the rat cerebellum: coexpression with AMPA receptors in parallel fiber-spine synapses and absence from climbing fiber-spine synapses. *J. Neurosci.*, **17**, 834–842.

McCormick, D.A. & Thompson, R.F. (1984) Cerebellum: essential involvement in the classically conditioned eyelid response. *Science*, **223**, 296–299.

Meathrel, K., Adamek, T., Batt, J., Rotin, D. & Doering, L.C. (2002) Protein tyrosine phosphatase σ-deficient mice show aberrant cytoarchitecture and structural abnormalities in the central nervous system. *J. Neurosci. Res.*, **70**, 24–35.

Miyakawa, T., Yared, E., Pak, J.H., Huang, F.L., Huang, K.P. & Crawley, J.N. (2001) Neurogranin null mutant mice display performance deficits on spatial learning tasks with anxiety related components. *Hippocampus*, **11**, 763–775.

Miyata, M., Kim, H.T., Hashimoto, K., Lee, T.K., Cho, S.Y., Jiang, H., Wu, Y., Jun, K., Wu, D., Kano, M. & Shin, H.S. (2001) Deficient long-term synaptic depression in the rostral cerebellum correlated with impaired motor learning in phospholipase Cβ4 mutant mice. *Eur. J. Neurosci.*, **13**, 1945–1954.

Moult, P.R., Gladding, C.M., Sanderson, T.M., Fitzjohn, S.M., Bashir, Z.I., Molnar, E. & Collingridge, G.L. (2006) Tyrosine phosphatases regulate AMPA receptor trafficking during metabotropic glutamate receptor-mediated long-term depression. *J. Neurosci.*, **26**, 2544–2554.

Namiki, S., Kakizawa, S., Hirose, K. & Iino, M. (2005) NO signalling decodes frequency of neuronal activity and generates synapse-specific plasticity in mouse cerebellum. *J. Physiol.*, **566**, 849–863.

Niisato, K., Fujikawa, A., Komai, S., Shintani, T., Watanabe, E., Sakaguchi, G., Katsuura, G., Manabe, T. & Noda, M. (2005) Age-dependent enhancement of hippocampal long-term potentiation and impairment of spatial learning through the Rho-associated kinase pathway in protein tyrosine phosphatase receptor type Z-deficient mice. *J. Neurosci.*, **25**, 1081–1088.

Nolan, M.F., Malleret, G., Lee, K.H., Gibbs, E., Dudman, J.T., Santoro, B., Yin, D., Thompson, R.F., Siegelbaum, S.A., Kandel, E.R. & Morozov, A. (2003) The hyperpolarization-activated HCN1 channel is important for motor learning and neuronal integration by cerebellar Purkinje cells. *Cell*, **115**, 551–564.

Petrone, A., Battaglia, F., Wang, C., Dusa, A., Su, J., Zagzag, D., Bianchi, R., Casaccia-Bonnefil, P., Arancio, O. & Sap, J. (2003) Receptor protein tyrosine phosphatase α is essential for hippocampal neuronal migration and long-term potentiation. *EMBO J.*, **22**, 4121–4131.

Safo, P.K. & Regehr, W.G. (2005) Endocannabinoids control the induction of cerebellar LTD. *Neuron*, **48**, 647–659.

Sahin, M., Slaugenhaupt, S.A., Gusella, J.F. & Hockfield, S. (1995) Expression of PTPH1, a rat protein tyrosine phosphatase, is restricted to the derivatives of a specific diencephalic segment. *Proc. Natl Acad. Sci. USA*, **92**, 7859–7863.

Sakimura, K., Kutsuwada, T., Ito, I., Manabe, T., Takayama, C., Kushiya, E., Yagi, T., Aizawa, S., Inoue, Y., Sugiyama, H. & Mishina, M. (1995) Reduced hippocampal LTP and spatial learning in mice lacking NMDA receptor ϵ1 subunit. *Nature*, **373**, 151–155.

Sakurai, M. (1990) Calcium is an intracellular mediator of the climbing fiber in induction of cerebellar long-term depression. *Proc. Natl Acad. Sci. USA*, **87**, 3383–3385.

Salter, M.W. & Kalia, L.V. (2004) Src kinases: a hub for NMDA receptor regulation. *Nat. Rev. Neurosci.*, **5**, 317–328.

Schmahmann, J.D. & Sherman, J.C. (1998) The cerebellar cognitive affective syndrome. *Brain*, **121**, 561–579.

Snyder, E.M., Nong, Y., Almeida, C.G., Paul, S., Moran, T., Choi, E.Y., Nairn, A.C., Salter, M.W., Lombroso, P.J., Gouras, G.K. & Greengard, P. (2005) Regulation of NMDA receptor trafficking by amyloid-β. *Nat. Neurosci.*, **8**, 1051–1058.

Steinberg, J.P., Takamiya, K., Shen, Y., Xia, J. & Rubio, M.E., Yu, S., Jin, W., Thomas, G.M., Linden, D.J. & Huganir, R.L. (2006) Targeted in vivo mutations of the AMPA receptor subunit GluR2 and its interacting protein PICK1 eliminate cerebellar long-term depression. *Neuron*, **49**, 845–860.

Swinny, J.D., van der Want, J.J. & Gramsbergen, A. (2005) Cerebellar development and plasticity: perspectives for motor coordination strategies, for motor skills, and for therapy. *Neural Plast.*, **12**, 153–160.

Tanaka, M., Maeda, N., Noda, M. & Marunouchi, T. (2003) A chondroitin sulfate proteoglycan PTPζ/RPTPβ regulates the morphogenesis of Purkinje cell dendrites in the developing cerebellum. *J. Neurosci.*, **23**, 2804–2814.

Thompson, R.F., Bao, S., Chen, L., Cipriano, B.D., Grethe, J.S., Kim, J.J., Thompson, J.K., Tracy, J.A., Weninger, M.S. & Krupa, D.J. (1997) Associative learning. *Int. Rev. Neurobiol.*, **41**, 151–189.

Thompson, R.F. & Kim, J.J. (1996) Memory systems in the brain and localization of a memory. *Proc. Natl Acad. Sci. USA*, **93**, 13438–13444.

Uetani, N., Kato, K., Ogura, H., Mizuno, K., Kawano, K., Mikoshiba, K., Yakura, H., Asano, M. & Iwakura, Y. (2000) Impaired learning with enhanced hippocampal long-term potentiation in PTPδ-deficient mice. *EMBO J.*, **19**, 2775–2785.

Wang, Y.T. & Linden, D.J. (2000) Expression of cerebellar long-term depression requires postsynaptic clathrin-mediated endocytosis. *Neuron*, **25**, 635–647.

Wansink, D.G., Peters, W., Schaafsma, I., Sutmuller, R.P., Oerlemans, F., Adema, G.J., Wieringa, B., van der Zee, C.E. & Hendriks, W. (2004) Mild impairment of motor nerve repair in mice lacking PTP-BL tyrosine phosphatase activity. *Physiol. Genomics*, **19**, 50–60.

Whited, J.L., Robichaux, M.B., Yang, J.C. & Garrity, P.A. (2007) Ptpmeg is required for the proper establishment and maintenance of axon projections in the central brain of Drosophila. *Development*, **134**, 43–53.

Yang, Q. & Tonks, N.K. (1991) Isolation of a cDNA clone encoding a human protein-tyrosine phosphatase with homology to the cytoskeletal-associated proteins band 4.1, ezrin, and talin. *Proc. Natl Acad. Sci. USA*, **88**, 5949–5953.

Yawata, S., Tsuchida, H., Kengaku, M. & Hirano, T. (2006) Membrane-proximal region of glutamate receptor δ2 subunit is critical for long-term depression and interaction with protein interacting with C kinase 1 in a cerebellar Purkinje neuron. *J. Neurosci.*, **26**, 3626–3633.

Yuzaki, M. (2004) The δ2 glutamate receptor: a key molecule controlling synaptic plasticity and structure in Purkinje cells. *Cerebellum*, **3**, 89–93.

© The Authors (2007). Journal Compilation © Federation of European Neuroscience Societies and Blackwell Publishing Ltd

Melanocortin 2 receptor is required for adrenal gland development, steroidogenesis, and neonatal gluconeogenesis

Dai Chida[a,b,c], Shinichi Nakagawa[d], So Nagai[e], Hiroshi Sagara[f], Harumi Katsumata[g], Toshihiro Imaki[g], Harumi Suzuki[b], Fumiko Mitani[h], Tadashi Ogishima[i], Chikara Shimizu[e], Hayato Kotaki[a], Shigeru Kakuta[a], Katsuko Sudo[a,j], Takao Koike[e], Mitsumasa Kubo[k,l], and Yoichiro Iwakura[a]

[a]Division of Cell Biology, Center for Experimental Medicine, and [f]Fine Morphology Laboratory, Department of Basic Medical Science, Institute of Medical Science, University of Tokyo, 4-6-1, Shirokanedai, Minato-ku, Tokyo 108-8639, Japan; [b]Department of Pathology, Research Institute, International Medical Center of Japan, 1-21-1, Toyama, Shinjuku-ku, Tokyo 162-8655, Japan; [d]Nakagawa Initiative Research Unit, Initiative Research Program, Frontier Research System, RIKEN, 2-1, Hirosawa, Wako, Saitama 351-0198, Japan; [e]Department of Medicine II, Hokkaido University Graduate School of Medicine, Kita 15, Nishi 7, Kita-ku, Sapporo 060-8638, Japan; [g]Department of Bioregulation, Institute of Development and Aging Sciences, Nippon Medical School, 1-396, Kosugi-cho, Nakahara-ku, Kawasaki-city, Kanagawa 211-8533, Japan; [h]Department of Biochemistry and Integrative Medical Biology, School of Medicine, Keio University, 35 Shinanomachi, Shinjuku-ku, Tokyo 160-8582, Japan; [i]Department of Chemistry, Faculty of Sciences, Kyushu University, Hakozaki 6-10-1, Higashi-ku, Fukuoka 812-8581, Japan; [j]Animal Research Center, Tokyo Medical University, 6-1-1, Shinjuku, Shinjuku-ku, Tokyo 160-8402, Japan; and [k]Health Administration Center, Hokkaido University of Education, 5-3-1, Ainosato, Kita-ku, Sapporo 002-8501, Japan

Edited by Richard D. Palmiter, University of Washington School of Medicine, Seattle, WA, and approved September 21, 2007 (received for review July 25, 2007)

ACTH (i.e., corticotropin) is the principal regulator of the hypothalamus–pituitary–adrenal axis and stimulates steroidogenesis in the adrenal gland via the specific cell-surface melanocortin 2 receptor (MC2R). Here, we generated mice with an inactivation mutation of the MC2R gene to elucidate the roles of MC2R in adrenal development, steroidogenesis, and carbohydrate metabolism. These mice, the last of the knockout (KO) mice to be generated for melanocortin family receptors, provide the opportunity to compare the phenotype of proopiomelanocortin KO mice with that of MC1R–MC5R KO mice. We found that the MC2R KO mutation led to neonatal lethality in three-quarters of the mice, possibly as a result of hypoglycemia. Those surviving to adulthood exhibited macroscopically detectable adrenal glands with markedly atrophied zona fasciculata, whereas the zona glomerulosa and the medulla remained fairly intact. Mutations of MC2R have been reported to be responsible for 25% of familial glucocorticoid deficiency (FGD) cases. Adult MC2R KO mice resembled FGD patients in several aspects, such as undetectable levels of corticosterone despite high levels of ACTH, unresponsiveness to ACTH, and hypoglycemia after prolonged (36 h) fasting. However, MC2R KO mice differ from patients with MC2R-null mutations in several aspects, such as low aldosterone levels and unaltered body length. These results indicate that MC2R is required for postnatal adrenal development and adrenal steroidogenesis and that MC2R KO mice provide a useful animal model by which to study FGD.

adrenocorticotropic hormone (ACTH) | familial glucocorticoid deficiency (FGD) | hypothalamus–pituitary–adrenal | zona fasciculata

The adrenal gland regulates a number of essential physiological functions in adult organisms through the production of steroids and catecholamines. Maintenance of adrenal structure and function is regulated through the integration of extra- and intracellular signals. The pituitary hormone ACTH (i.e., adrenocorticotropic hormone), which is derived from the proopiomelanocortin (POMC) polypeptide precursor, is the principal regulator that stimulates adrenal glucocorticoid (GC) biosynthesis and secretion via the membrane-bound specific receptor for ACTH, ACTH receptor/melanocortin 2 receptor (MC2R) (1).

It was previously demonstrated that, although POMC knockout (KO) mice are born at the expected Mendelian frequency, three-quarters of POMC KO mice undergo neonatal death. Furthermore, those mice surviving to adulthood exhibit obesity, pigmentation defects, and adrenal insufficiency (2–4). POMC KO mice possess macroscopically detectable adrenal glands that lack normal architecture (2, 4, 5). These results demonstrate the importance of POMC-derived peptides in regulating the hypothalamus–pituitary–adrenal axis and adrenal development.

Familial glucocorticoid deficiency (FGD), or hereditary unresponsiveness to ACTH [Online Mendelian Inheritance in Man (OMIM) no. 202200; www.ncbi.nlm.nih.gov/entrez/dispomim.cgi?id=202200], is an autosomal recessive disorder resulting from resistance to the action of ACTH on the adrenal cortex. Affected individuals are deficient in cortisol and, if untreated, are likely to die as a result of hypoglycemia or overwhelming infection in infancy or childhood (6). Mutations of MC2R are responsible for 25% of FGD cases. Mutations of the MC2R accessory protein MRAP, which plays a role in the trafficking of MC2R from the endoplasmic reticulum to the cell surface, account for 20% of FGD cases (7), and a third locus responsible for FGD has been suggested (8). There has been no animal model for FGD, and MC2R KO mice are likely to become a valuable tool for the pathophysiological investigation of FGD.

To study specifically the roles of MC2R in adrenal gland development, steroidogenesis, and carbohydrate metabolism, we generated mice with an inactivation mutation of the MC2R gene. We demonstrated that disruption of MC2R leads to neonatal lethality in approximately three-quarters of MC2R KO pups, possibly as a result of hypoglycemia. Those surviving to adulthood exhibited macroscopically detectable adrenal glands with markedly atrophied zona fasciculata (zF) and lack of detectable levels of GC and reduced serum concentrations of aldosterone and epinephrine. Those surviving to adulthood exhibited hypoglycemia after prolonged (36 h) fasting as a result of the reduced expression of the genes involved in gluconeogenesis.

Author contributions: D.C., T.K., M.K., and Y.I. designed research; D.C., S. Nakagawa, S. Nagai, H. Sagara, H. Katsumata, T.I., C.S., H. Kotaki, S.K., K.S., and M.K. performed research; H. Suzuki, F.M., and T.O. contributed new reagents/analytic tools; D.C., S. Nakagawa, H. Sagara, T.I., F.M., M.K., and Y.I. analyzed data; and D.C. and M.K. wrote the paper.

The authors declare no conflict of interest.

This article is a PNAS Direct Submission.

Abbreviations: ACTH, adrenocorticotropic hormone; POMC, proopiomelanocortin; GC, glucocorticoid; KO, knockout; FGD, familial glucocorticoid deficiency; zF, zona fasciculata; zG, zona glomerulosa; ME, medulla; TH, tyrosine hydroxylase.

[c]To whom correspondence should be sent at the b address. E-mail: dchida@ri.imcj.go.jp.

[l]Deceased January 21, 2007.

This article contains supporting information online at www.pnas.org/cgi/content/full/0706953104/DC1.

© 2007 by The National Academy of Sciences of the USA

MEDICAL SCIENCES

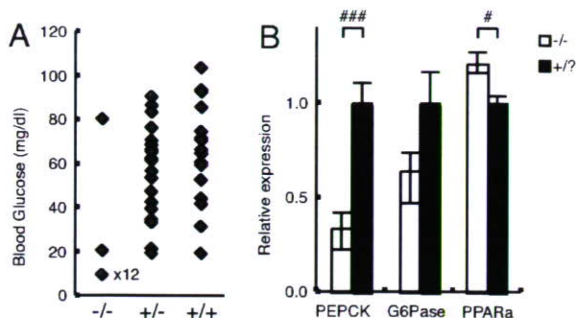

Fig. 1. Neonatal hypoglycemia in MC2R KO mice. (*A*) Blood glucose levels on postnatal day 0.5 at 1200 hours. Detection limit was 20 mg/dl. Each point indicates the glucose level of a single pup. The blood glucose level of 12 of 14 homozygous pups was under detection level (<20 mg/dl). The values below detection level were plotted at 10 mg/dl. (*B*) MC2R pups were killed at 1200 hours, and liver RNAs were prepared. The experiments were performed with postnatal day 0.5 MC2R$^{-/-}$ (n = 6) and MC2R$^{+/?}$ (n = 9) mice. The expression of phospho*enol*pyruvate carboxykinase (PEPCK), glucose-6-phosphatase (G6Pase), and peroxisome proliferator-activated receptor α (PPARa) in the liver was determined by qRT-PCR. Data are expressed as means ± SEM. Statistical significance was determined by *t* test. #, $P < 0.05$.

Results

Generation of MC2R KO Mice. To generate MC2R KO mice, a targeting vector was constructed in which the portion of the MC2R gene encoding the entire coding region (9) was replaced with a neomycin-resistance gene cassette [supporting information (SI) Fig. 7*A*]. One of 545 neomycin-resistant colonies screened was positive as assessed by Southern analysis with an external probe (Fig. 7*B*). Chimeric founder mice were produced from the targeted ES cell clones, and germ-line transmission of the disrupted allele was obtained. MC2R KO mice were back-crossed to C57BL/6J mice for five generations before use in this study. To confirm the deficiency of MC2R, expression of the MC2R gene in the adrenal gland was examined by quantitative real-time PCR (qRT-PCR). No mRNA was detected in MC2R$^{-/-}$ mice, and expression was decreased by approximately half in MC2R$^{+/-}$ mice (Fig. 7*C*).

Most of the MC2R KO Pups Died Shortly After Birth. Mice that were homozygous null for MC2R were obtained by interbreeding heterozygous mice. Pups lacking MC2R were born at the expected Mendelian ratio, suggesting that MC2R is not essential for embryonic development. Of 190 mice born from heterozygous MC2R KO parents, 61 pups were dead before weaning at 4 wk of age. Genotype analysis revealed that most of the 61 dead pups were homozygous for the MC2R allele. Genotype analysis of 129 mice at 4 wk revealed 9 homozygote, 74 heterozygote, and 46 WT mice. Approximately three-quarters of MC2R KO pups died before weaning, mostly within 48 h after birth. Most of the mutant newborn mice were indistinguishable from their WT littermates; some homozygous pups were pink and had milk in their stomachs, whereas some homozygous pups were lethargic and pale.

We analyzed blood glucose levels on postnatal day 0.5 at 1200 hours. Three of 57 mice had already died at the time of analysis (two were MC2R$^{-/-}$ and one was MC2R$^{+/-}$). MC2R$^{-/-}$ pups were significantly hypoglycemic compared with MC2R$^{+/?}$ pups (Fig. 1*A*). We found only one of 14 homozygous pups that maintained normal blood glucose levels, comparable with those in WT mice. It is possible that this pup could survive neonatal death and grow to adulthood. Blood glucose levels for 12 of 14 homozygous pups were below detection level (<20 mg/dl). Analysis of blood glucose levels on postnatal day 7 revealed that MC2R$^{-/-}$ pups maintained glucose levels comparable with those of WT mice (data not shown). Expression of phosphoenolpyruvate carboxykinase (PEPCK), a rate-limiting enzyme for gluconeogenesis in liver, was significantly decreased, and expression of glucose-6-phosphatase (G6Pase) was relatively decreased in MC2R KO pups compared with MC2R$^{+/?}$ pups (Fig. 1*B*). The expression of peroxisome proliferator-activated receptor α (PPARα) responsible for β-oxidation of free fatty acids was significantly increased in MC2R KO pups (Fig. 1*B*). These results suggest that MC2R KO mice die as a result of hypoglycemia with decreased gluconeogenesis in the liver and defective neonatal nutritional adaptation. A slight increase in mortality was observed at 3–4 wk of age, due to undetermined cause(s), but no increase in mortality was observed after that period.

The body weights of 12-wk-old MC2R KO mice were indistinguishable from those of their littermates: MC2R$^{-/-}$, 28.7 ± 0.8 g (n = 4); and MC2R$^{+/+}$, 28.8 ± 0.6 g (n = 5). Whereas FGD patients with MC2R mutations exhibited increased height and POMC KO mice exhibited increased body length (10, 11), MC2R KO mice did not exhibit any significant difference in body length compared with that of their WT siblings: MC2R$^{-/-}$, 9.58 ± 0.17 cm (n = 5); and MC2R$^{+/?}$, 9.74 ± 0.07 cm (n = 10).

Adrenal Hypoplasia in MC2R KO Mice That Survived to Adulthood. In MC2R KO mice, adrenal glands were considerably reduced in size compared with those of their WT siblings: male MC2R$^{-/-}$, 0.58 ± 0.02 mg per pair of glands (n = 4); and MC2R$^{+/+}$, 2.24 ± 0.18 mg per pair of glands (n = 5). The histological analysis revealed marked hypoplasia of zF in the mutant adrenal gland (Fig. 2*A*). The number of nuclei per 50-μm-wide column in the cortical area, however, was not significantly changed: male MC2R$^{+/-}$, 138.2 ± 13.3; and MC2R$^{-/-}$, 147.7 ± 19.8, $P > 0.35$; and female MC2R$^{+/-}$, 149.7 ± 18; and MC2R$^{-/-}$, 143.8 ± 20.7, $P > 0.61$. These results indicate that the total number of nuclei in the zF was similar in MC2R KO and WT mice. Higher-magnification images revealed that, in the MC2R KO mice, the nuclei in zF were more densely packed with reduced cytoplasmic volume (Fig. 2*B*), suggesting that a decrease in cell size, but not cell number, accounted for the hypoplasia of zF. On the other hand, the zona glomerulosa (zG) and the adrenal medulla (ME) remained fairly intact as shown in the histological sections (Fig. 2*B*). To confirm this idea, we examined the expression patterns of aldosterone synthase cytochrome P450 (P450aldo) and tyrosine hydroxylase (TH), markers for zG and ME, respectively. Both of these markers were similarly expressed in WT and MC2R KO mice (Fig. 2*C*), suggesting that the cells in zG and ME had differentiated into the appropriate cell types. We also noticed that the thickness of capsule was increased in MC2R KO mice (Fig. 2*B*, brackets).

Ultrastructural examination of zF cells in MC2R KO mice revealed that the number of lipid droplets was significantly decreased and mitochondrial appearance was inactive compared with that of WT mice (Fig. 3 *B* and *D*). In contrast, zG cells in MC2R KO mice contained lipid droplets comparable with those in WT mice, and zG cells were not significantly different from those of WT mice (Fig. 3 *A* and *C*). Chromaffin cells in MC2R KO mice exhibited a marked depletion in epinephrine-storing secretory granules (data not shown), and highly vascularized connective tissue was developed in MC2R KO adrenal ME (data not shown). The H&E staining of the adrenal glands of newborn (postnatal day 0.5) MC2R KO mice was not significantly different from that of WT siblings (data not shown), suggesting that postnatal adrenal development was impaired in MC2R KO mice.

Adrenal Hormones in MC2R KO Mice. Serum corticosterone levels in MC2R KO mice were undetectable (Fig. 4*A*): male MC2R$^{-/-}$, undetectable (n = 4); MC2R$^{+/-}$, 72.0 ± 8.9 ng/ml (n = 6); and MC2R$^{+/+}$, 59.0 ± 8.6 ng/ml (n = 5). ACTH levels were significantly increased in MC2R KO mice (Fig. 4*B*): male MC2R$^{-/-}$, 1,394 ± 89 pg/ml (n = 4); MC2R$^{+/-}$, 370 ± 50 pg/ml (n = 6); and MC2R$^{+/+}$,

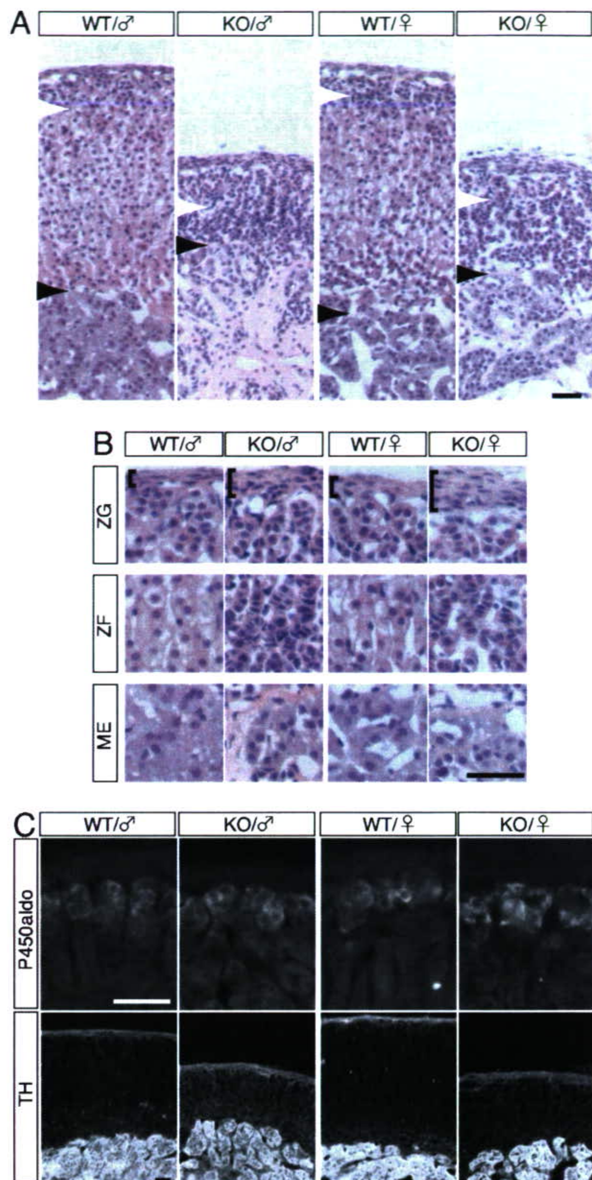

Fig. 2. Histological analysis of the adrenal gland of MC2R KO mice. (*A* and *B*) H&E staining of sections from the adrenal gland of WT or MC2R KO mice. Ten-week-old male or 13-wk-old female WT and MC2R KO mice were analyzed. (*B*) Higher-magnification images of zG, zF, and ME shown in *A*. The white and black arrowheads in *A* indicate the border between zG/zF and cortical zone/ME, respectively. The brackets in *B* indicate thickness of the capsule, which was remarkably thicker in the mutant mice. (*C*) Immunofluorescent detection of aldosterone synthase cytochrome P450 (P450aldo) and TH in the adrenal gland of WT and MC2R KO mice. Both enzymes were normally expressed in the mutant mice. (Scale bars, 50 μm.)

281 ± 106 pg/ml (n = 5). Surprisingly, serum aldosterone levels were significantly decreased in MC2R KO mice (Fig. 4*C*): male $MC2R^{-/-}$, 104 ± 25 pg/ml (n = 4); and $MC2R^{+/+}$, 343 ± 103 pg/ml (n = 5). In this regard, the MC2R-deficient mouse model is different from patients with MC2R-null mutations, in whom there is no mineralocorticoid deficiency and the renin–angiotensin system (RAS) is not affected (OMIM no. 202200). Consistent with the reduced serum corticosterone in MC2R KO mice, thymus and spleen weights were significantly increased and adipose weight was significantly decreased compared with those of WT mice (data not shown).

We analyzed the corticosterone response to exogenously

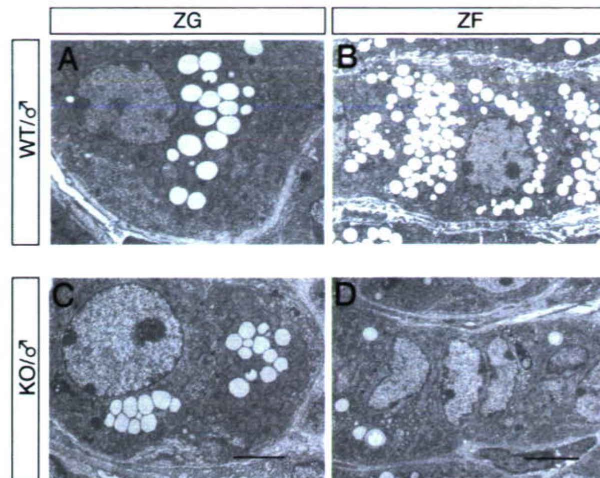

Fig. 3. Electron micrographs of the adrenal gland from MC2R KO mice. (*A* and *C*) Electron micrographs of zG of WT or MC2R KO mice. (Scale bars, 2 μm.) (*B* and *D*) Electron micrographs of zF of WT or MC2R KO mice. (Scale bars, 5 μm.) Note the remarkable decrease in lipids in zF in MC2R KO mice.

administered ACTH in MC2R KO mice. The responsiveness to ACTH was completely abrogated in MC2R KO mice (Fig. 4*E*): male $MC2R^{-/-}$, ACTH, undetectable (n = 8); $MC2R^{+/-}$, saline, 80.1 ± 13.8 ng/ml (n = 11), and ACTH, 233.9 ± 46.6 ng/ml (n = 11); and $MC2R^{+/+}$, saline, 75.2 ± 20.9 ng/ml (n = 5), and ACTH, 186.9 ± 37.6 ng/ml (n = 8). These results indicate that MC2R is essential for corticosterone release in response to ACTH.

Because ACTH plays an essential role in regulating 11β-hydroxylase (Cyp11b1) expression, as well as other genes encoding enzymes involved in steroidogenesis (12), we analyzed the expression of adrenal steroidogenic enzymes. Expression levels of cholesterol side-chain cleavage enzyme P450scc (Cyp11a1) (Fig. 5*A*), Cyp21a1 (Fig. 5*B*), and Cyp11b1 (Fig. 5*C*) were significantly reduced in MC2R KO mice, reflecting the hypoplasia of zF. The expression of Cyp11b2 [aldosterone synthase (P450aldo)] was relatively reduced in adrenal glands from MC2R KO mice (Fig. 5*D*). These results collectively indicate that the reduction of corticosterone level (Fig. 4*A*) is due to hypoplasia of zF with reduced lipid droplets (Figs. 2*A* and 3*C*), together with reduced levels of Cyp11b1 and rate-limiting Cyp11a1 (Fig. 5 *A* and *C*).

To determine the physiological effect of reduced aldosterone levels in MC2R KO mice, we measured serum electrolytes and blood pressure at 12 wk of age. There were no differences in the sodium concentrations of MC2R KO and WT mice, whereas chloride levels increased significantly in male MC2R KO mice and tended to increase in female MC2R KO mice (data not shown). Female MC2R KO mice exhibited significantly increased potassium levels (data not shown), whereas male MC2R KO mice did not. Although no significant differences in blood pressure were observed, the heart rate was significantly attenuated in MC2R KO mice (data not shown), consistent with reduced epinephrine levels in MC2R KO mice (Fig. 4*D*). We found that the expression of angiotensin receptor 1b (AT1bR) was significantly increased in MC2R KO mice (Fig. 5*E*), suggesting that renin–angiotensin system (RAS) signaling was enhanced in MC2R KO glomerulosa cells to compensate for the complete absence of ACTH signaling.

Measurement of catecholamine levels demonstrated that epinephrine levels were significantly reduced (Fig. 4*D*): male $MC2R^{-/-}$, 0.12 ± 0.02 ng/ml (n = 4); $MC2R^{+/-}$, 0.72 ± 0.14 ng/ml (n = 6); and $MC2R^{+/+}$, 0.59 ± 0.08 ng/ml (n = 5). However, norepinephrine and dopamine levels were not signif-

MEDICAL SCIENCES

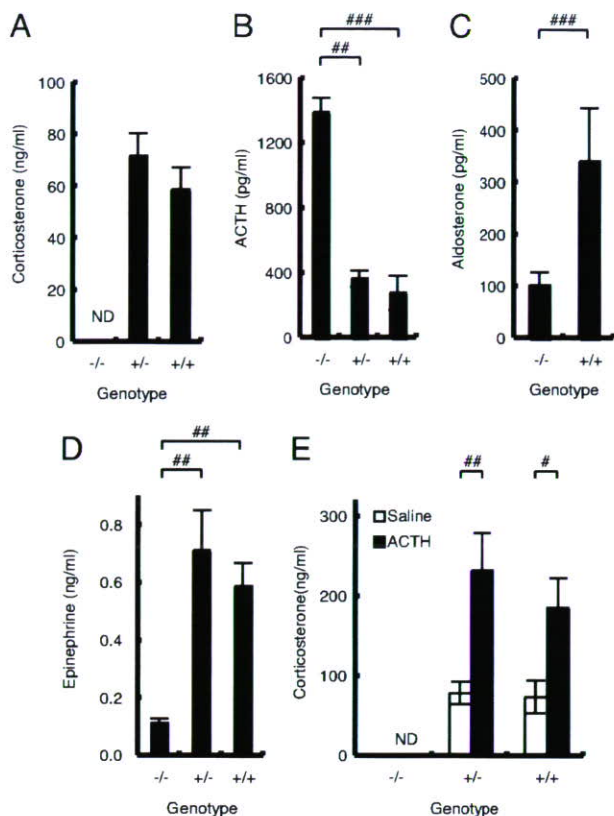

Fig. 4. Hormone levels in MC2R KO mice. (*A–D*) Blood was collected at 1600 hours from male mice (male $MC2R^{-/-}$, $n = 4$; $MC2R^{+/-}$, $n = 6$; and $MC2R^{+/+}$, $n = 5$) fasted for 8 h. Serum corticosterone (*A*), ACTH (*B*), aldosterone (*C*), and epinephrine (*D*) levels were determined. (*E*) Serum corticosterone response after ACTH (10 μg per kg of body weight) or saline injection in 12-wk-old male $MC2R^{-/-}$ [saline, not determined (ND); ACTH, $n = 8$], $MC2R^{+/-}$ (saline, $n = 11$; ACTH, $n = 11$), or $MC2R^{+/+}$ (saline, $n = 5$; ACTH, $n = 8$) mice. ACTH or saline was injected from 1000 to 1030 hours, and blood was collected after 60 min. Data are expressed as means ± SEM. Statistical significance was determined by one-way ANOVA and Fisher's protected least significant difference (PLSD) test (*A, B, D*, and *E*) or *t* test (*C*). ###, $P < 0.001$; ##, $P < 0.01$; #, $P < 0.05$.

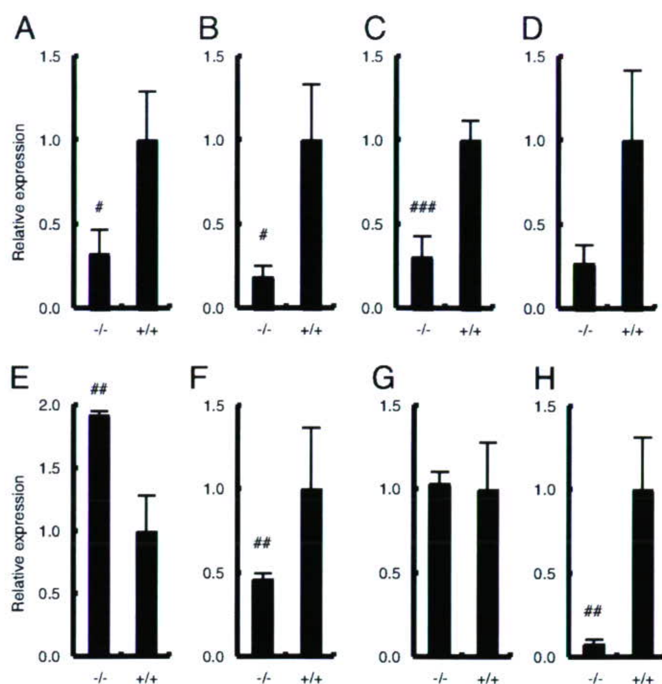

Fig. 5. Adrenal gene expression in MC2R KO mice. Expression of Cyp11a1 (*A*), Cyp21a1 (*B*), Cyp11b1 (*C*), Cyp11b2 (*D*), AT1bR (*E*), TH (*F*), Phox2a (*G*), and phenylethanolamine *N*-methyltransferase (PNMT) (*H*) in adrenal glands from female 12-wk-old $MC2R^{-/-}$ ($n = 4$) and $MC2R^{+/+}$ ($n = 3$) mice was determined by qRT-PCR. Data are expressed as means ± SEM. Statistical significance was determined by *t* test. ###, $P < 0.001$; ##, $P < 0.01$; #, $P < 0.05$.

icantly altered in MC2R KO mice (data not shown). The expression of TH was significantly reduced in MC2R KO adrenal glands (Fig. 5*F*), whereas the expression of Phox2a, a specific marker for chromaffin cells, was not significantly different (Fig. 5*G*), suggesting that MC2R is not required for chromaffin cell development but is necessary for TH expression. These results are consistent with a previous report that GC is not required for chromaffin cell development (13). We also observed that the expression of phenylethanolamine *N*-methyltransferase (PNMT), which catalyzes the conversion of norepinephrine to epinephrine and is modulated by GC, was significantly reduced in adrenal glands from MC2R KO mice (Fig. 5*H*). These results suggest that the reduced epinephrine level in MC2R KO mice is due to the reduced expression levels of PNMT and TH.

MC2R KO Mice Develop Hypoglycemia upon Prolonged Fasting. We measured blood glucose levels in animals both fed and fasted for 8 h. Interestingly, adult MC2R KO mice exhibited relatively higher glucose levels than those of WT mice under fed and 8-h fasting conditions. However, the difference was not statistically significant (data not shown). MC2R KO mice exhibited relatively reduced serum insulin levels compared with control littermates. However, the difference was not statistically significant: male $MC2R^{-/-}$, 2,044 ± 190 pg/ml ($n = 4$); and $MC2R^{+/+}$, 2,644 ± 265 pg/ml ($n = 5$).

We next evaluated the role of MC2R during prolonged starvation. After 36 h of starvation, liver gluconeogenesis becomes the major source of blood glucose (14). During a 36-h fast, MC2R KO mice exhibited a faster decline in blood glucose levels (Fig. 6*A*): male $MC2R^{-/-}$, 45.8 ± 11.7 mg/dl ($n = 5$); and $MC2R^{+/+}$, 79.2 ± 9.5 mg/dl ($n = 5$). As anticipated, corticosterone levels in WT mice were increased in response to fasting, whereas corticosterone levels in MC2R KO mice were not increased in response to a 36-h fast (Fig. 6*B*): male $MC2R^{-/-}$, undetectable ($n = 5$); and $MC2R^{+/+}$, 94.4 ± 23.4 ng/ml ($n = 5$). Serum epinephrine was significantly decreased in MC2R KO mice, whereas norepinephrine, dopamine, insulin, and glucagon levels (data not shown) were not significantly different. The expression of PEPCK, which is a rate-limiting enzyme in gluconeogenesis, was significantly decreased, and G6Pase was relatively decreased in MC2R KO mice after a prolonged (36 h) fast (Fig. 6*C*), indicating that the lower blood glucose levels in MC2R KO mice were due to impaired gluconeogenesis.

Discussion

Immediately after birth, the maternal supply of substrates ceases abruptly, and the newborn mouse has to withstand a brief period of starvation before being fed with milk that is high in fat and low in carbohydrates. The adaptation of neonates to these changes in nutrition and environment requires modification of glucose and fatty acid metabolism, which is controlled by the neonatal increase in glucagon and the fall in insulin (15). Defective gluconeogenesis leads to neonatal death (16). Plasma corticosterone levels are high at delivery and rapidly decline during the first 24 h after birth, and epinephrine and norepinephrine levels are increased severalfold in newborns in response to the stresses of birth, such as transient hypoxia, cold exposure, and cord cutting (15). Because GC plays a critical role in the maintenance of neonatal blood glucose levels through the induction of

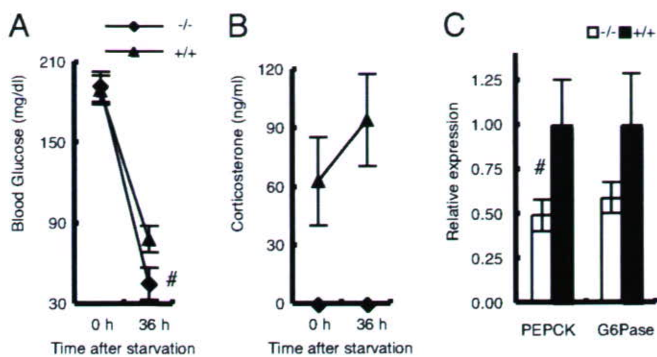

Fig. 6. MC2R KO mice develop hypoglycemia during fasting. The experiment was performed with 12-wk-old male MC2R$^{-/-}$ (n = 5) and MC2R$^{+/+}$ (n = 5) mice. (*A* and *B*) At time 0 (2000 hours), food was withdrawn and blood glucose (*A*) and serum corticosterone level (*B*) were measured. After 36 h, mice (at 0800 hours) were killed and serum samples and liver RNA were prepared. Expression of phospho*enol*pyruvate carboxykinase (PEPCK) and glucose-6-phosphatase (G6Pase) in the liver was determined by qRT-PCR (*C*). Data are expressed as means ± SEM. The statistical difference was evaluated by two-way ANOVA (factor 1 was genotype and factor 2 was treatment) followed by *t* test to compare the significant difference between the glucose value for 36 h of MC2R KO mice and the glucose value for 36 h of WT mice. #, $P < 0.05$.

gluconeogenesis, one-half of hepatocyte-specific GC receptor KO mice die shortly after birth as a result of hypoglycemia (17). Here, we demonstrated that MC2R KO mice are defective in this adaptation, consistent with a previous report that 75% of POMC KO mice die shortly after birth (2). Genetic replacement of pituitary POMC in POMC KO mice (POMC$^{-/-}$Tg^{+}) rescues neonatal lethality in POMC KO mice, suggesting that peripheral POMC, possibly ACTH, is important for neonatal survival (18). These results collectively suggest that ACTH MC2R signaling plays a critical role in the neonatal adaptation to nutrition supply, consistent with the fact that patients with FGD often suffer from neonatal hypoglycemia (OMIM no. 202200) (19). Neonatal hypoglycemia in MC2R KO mice might be secondary to low levels of both circulating corticosterone and epinephrine. It is also interesting that a slight increase in mortality was also observed at 3–4 wk of age because weaning is a crucial period when mice need to adapt to nutritional modifications. In fact, corticosterone concentration is low during the suckling period, increases after 12 days, and peaks at 24 days (15). Further studies are required to clarify the possible role of ACTH MC2R in suckling/weaning adaptation.

We observed significant adrenocortical hypoplasia in adult MC2R KO mice compared with WT siblings. Although zG cells remained fairly intact, zF cells were severely atrophied (Fig. 2), indicating that MC2R is not required for proper development of zG cells but is required for that of zF cells. Adrenal glands of rodents possess a transient zone between the adrenal cortex and the adrenal ME called the murine X zone. The overall function of the X zone remains unclear (20). Detailed studies are required to clarify the possible effect of ACTH deficiency on X zone regression. Because the adrenal glands from MC2R KO pups were indistinguishable in size and histological appearance from those from WT littermates at birth (data not shown), consistent with POMC KO mice (21), the ACTH MC2R signaling pathway regulates postnatal development of the adrenal gland. It was previously proposed that POMC-derived peptides other than ACTH contribute to adrenal development, function, and maintenance. Specifically, cleavage of the N-terminal POMC (amino acids 1–74) results in the generation of shorter peptides with mitogenic properties (22). If POMC-derived peptides other than ACTH have any role in adrenal development, the adrenal phenotype of MC2R KO mice should be less severe than that of POMC KO mice. Compared with the adrenal structure of POMC KO mice previously reported (2, 4), the adrenal structure/morphology of MC2R KO mice was intact, especially in zG. The total number of nuclei in zF of MC2R KO mice was not significantly changed (Fig. 2*A*), suggesting that the proliferation of zF in MC2R KO mice was comparable with that in WT mice. In contrast, it was previously demonstrated that adrenal glands of POMC KO mice on postnatal day 14 had reduced proliferating cell nuclear antigen (PCNA)-positive cells (21). These differences could be explained by the possible role of POMC-derived peptides other than ACTH in adrenal development (22), although we could not exclude the possibility of difference due to genetic background or of compensatory function by other MCRs in the absence of MC2R. Simultaneous comparison of POMC KO mice and MC2R KO mice is required to clarify these possibilities.

We analyzed the adrenal gene expression involved in the syntheses of corticosterone, aldosterone, and catecholamines in MC2R KO mice at 12 wk of age. Two previous studies have shown adrenal gene expression profiles in POMC KO mice. Karpac *et al.* (21) demonstrated that the expression of Cyp11b2, Cyp11b1, and TH in POMC KO mice at 5 wk of age was not significantly different from that in WT mice and suggested that the essential role for POMC peptides is in the maintenance of the adrenal gland and not in differentiation. Coll *et al.* (23) also analyzed the expression of Cyp11b1 and Cyp11a1 and demonstrated that the expression of both was reduced in POMC KO mice at 8 wk of age. Although the latter results were consistent with ours, the former results were not. We could not fully explain the reason for the difference: however, one possible explanation is that adrenal glands of POMC KO and MC2R KO mice at 5 wk of age are indistinguishable from those of WT mice and that they regress thereafter, as suggested by Karpac *et al.* (21). Further developmental studies on the adrenal gland in POMC KO and MC2R KO mice are needed to clarify these issues.

We found that the adrenal glands in MC2R KO mice produce aldosterone at reduced levels, as has been observed in POMC KO mice (2, 4). In this regard, the MC2R-deficient mouse model is different from FGD type 1 patients, who have been reported to exhibit normal serum aldosterone levels (24). This disparity could be explained by the fact that the majority of humans have one or two missense alleles, and homozygous nonsense mutations are very rare. It was recently reported that a small number of such patients may provide biochemical evidence of mineralocorticoid deficiency (25). The role of ACTH in aldosterone production is further supported by the fact that glucocorticoid receptor (GR) KO mice had enlarged adrenal glands with greatly increased expression of not only Cyp11b1 but also Cyp11b2 at embryonic day 18.5 (26). GR KO mice had increased ACTH levels as a result of the deficiency of negative feedback by corticosterone (26). It is possible that increased ACTH levels in GR KO mice are directly responsible for the increased expression of Cyp11b2 in zG. These observations collectively indicate that ACTH MC2R signaling is an important regulator of aldosterone production.

Here we described the initial characterization of MC2R KO mice and confirmed and extended the importance of ACTH-MC2R in neonatal adaptation to nutrition supplies, adrenal development, and the production of corticosterone and aldosterone. The possible role of ACTH-MC2R in adipose metabolism (27), β-cell function (28), and skin homeostasis (29) could be clarified by further analysis of MC2R KO mice.

Materials and Methods

Animals. Generation of MC2R KO mice is described in *SI Materials and Methods*. For analysis of tissue weight, 12-wk-old mice of each genotype were evaluated. Adrenal glands were dissected, cleaned of fat under a stereoscopic microscope, and

MEDICAL SCIENCES